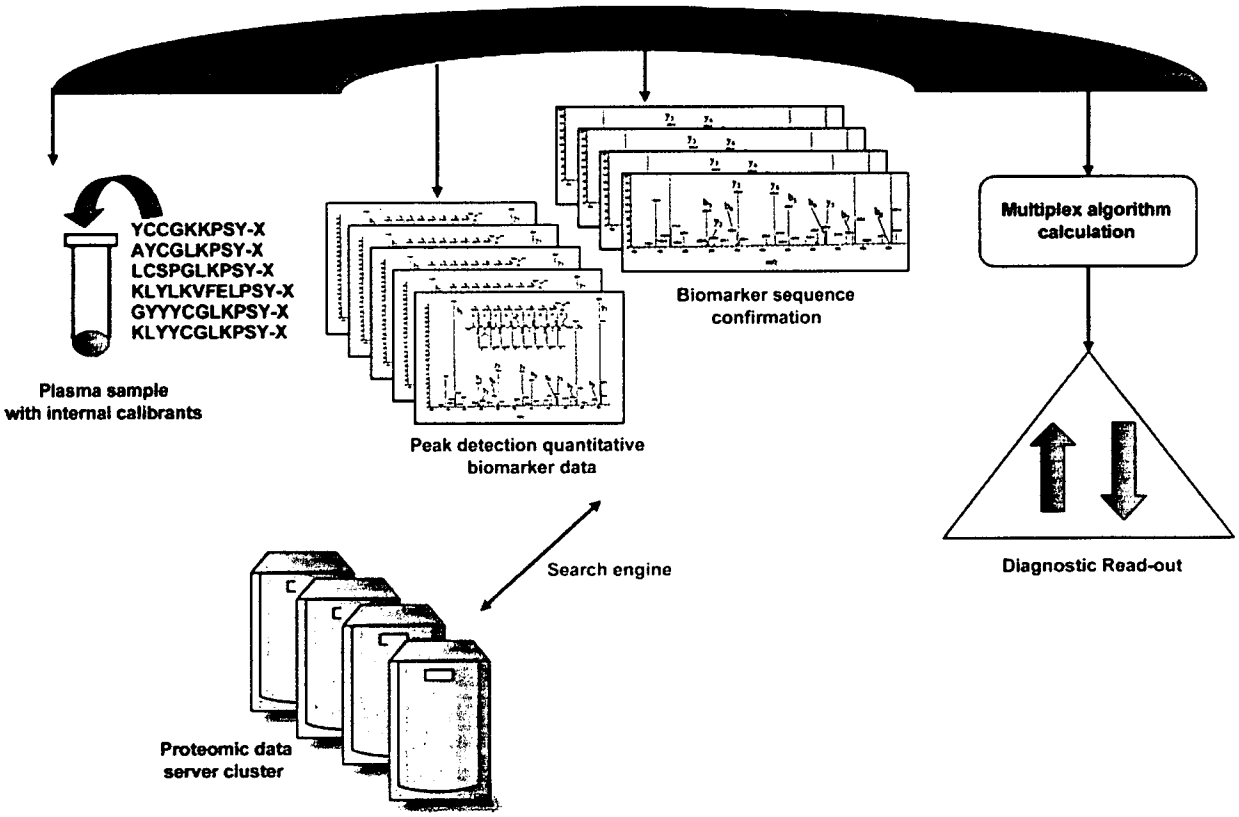

Figure 5. Entire flow of the operational components of Mass Spectrometric Biomarker Assays (MSBA).

The MSBA builds on a pre-defined Multiplex Biomarker list, which is stored within the MSBA database. Each marker entity has the values of masses and the relative retention time index with tolerance parameters. In running a patient sample, the predefined biomarker list is scanned to pick up patient sample signals that match with one of the predefined biomarker signals by satisfying the tolerance criteria (in general ±1 for m/z value and ±2% for relative retention time index). The selected candidate signals are further confirmed using the product ion spectrum. That is, the product ion spectrum is represented as a vector by binning (grouping) the m/z ratio values. Using the cosine correlation between the sample vectors and the reference vectors, we can confirm whether the selected candidate signals are truly assigned as target biomarkers. (A standard threshold value of the cosine correlation is 0.8.)

The process steps within the MSBA cycle are outlined in Figure 5. The calculation of the final multiplex biomarker assay read-out from all of the individual markers can be performed by a variety of applications, as discussed in more detail in the Principled Statistical Modeling Approach section. Figures 6A and B illustrate one approach, calculating a distance score which indicates to what extent a measured sample is distant from the case or control template in terms of predefined multiplex biomarkers.

$$S_{\substack{\text{case or}\\ \text{control}}} = \sqrt{\left[\frac{1}{n(n-2)}\right]\left[n\sum_i y_i^2 - \left(\sum_i y_i\right)^2 - \frac{\left[n\sum_i x_i y_i - \left(\sum_i x_i\right)\left(\sum_i y_i\right)\right]^2}{n\sum_i x_i^2 - \left(\sum_i x_i\right)^2}\right]}$$

If the ratio of S_{case} and S_{control} exceeds an MSBA threshold parameter, then the test sample is predicted to be a patient susceptible to develop ILD (ILD case); if not, the test sample is predicted to be a non-susceptible patient (control). We are currently evaluating the MSBA approach in practice.

A Principled Statistical Modeling Approach

We have described an analytical approach based on proteomic data, with various novel developments. However, additional insight is needed to further improve model discrimination and to broaden the focus from the proteomic data to the ultimate goal of prediction using combinations of data. Statistical analysis can be used to provide further refinement by combining information from the full clinical and laboratory datasets.

An advantage of a multiple biomarker approach (e.g., proteomics) compared with standard single biomarker development is the capability to combine information from many different entities. An example is illustrated in Figure 7A. Considering each biomarker alone fails to separate the two groups of subjects, as there is considerable overlap for both biomarkers. Use of two biomarkers in combination completely separates the two groups.

We can also use clinical variables to advantage in the analysis of the peptide patterns. For example, the efficacy of gefitinib appears to be greater in non-smokers, women, patients of Asian origin, and patients with adenocarcinomas.[8] Figure 7B illustrates how, instead of two protein biomarkers, the combination of clinical data (e.g., age) and a proteomic biomarker is able to separate two groups.

On this basis, we propose using a principled statistical analysis approach to first explore and understand the data and

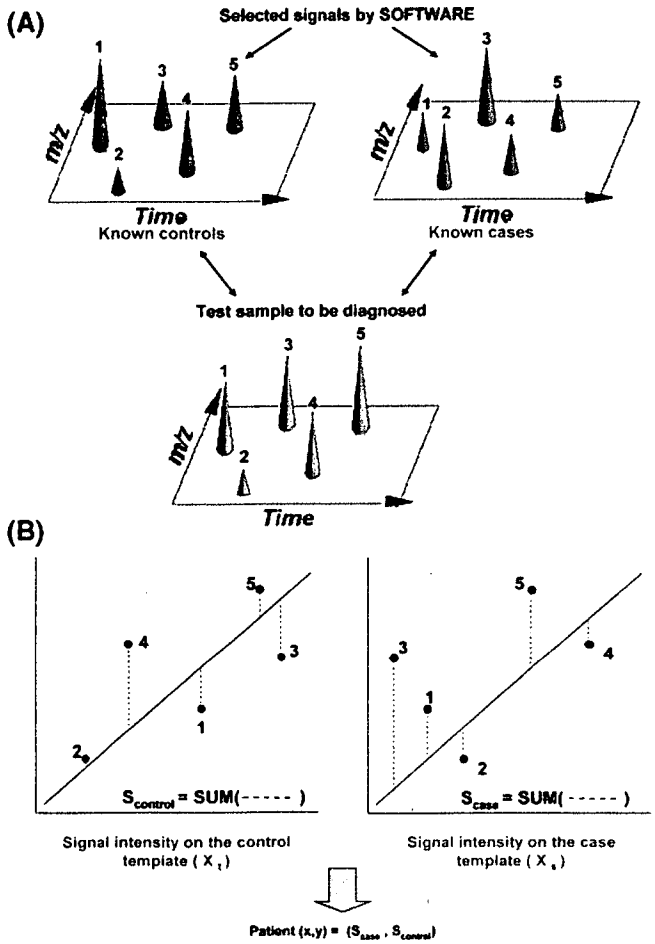

Figure 6. (A) Peptide signal comparison that MSBA (Mass Spectrometric Biomarker Assays) performs of the generated ions from the sample. The comparison is made both with the pattern of the controls and with the pattern of the case group for the corresponding signals. (B) Illustration of the regression model application of the MSBA where control templates and case templates are compared to that of the sample template generated in the analysis process.

then to model it and understand the quality of any models produced. A first step is to perform exploratory data analysis (EDA), for example using principal components analysis (PCA), to understand the major sources of data variation and the covariation between clinical parameters and protein intensity measures. The next step is univariate modeling for each protein marker individually, for example using analysis of covariance (ANCOVA), and an assessment of the effect of clinical parameters across the whole set of protein biomarkers using, for example, the False Discovery Rate as a tool.[75] This provides an understanding of key clinical variables and sources of variation within the data.

The next step is to perform multivariate predictive modeling using the proteins and clinical variables identified as being potentially important. There are a number of mathematical methods described in the literature for performing supervised classification, for example Support Vector Machines,[76] Random Forests,[77] PAM,[78] all of which have been successfully applied to high dimensional genomics data.[79] It remains an important unanswered question which modeling approach, or combination of modeling approaches, will generate the most predictive and robust models for data generated using this technology within a prospective study of this design.

Finally, to confirm that we have a practical prediction, the predictive power of a model must be assessed on a different set of patients from that used to generate the model. There are a number of approaches for external validation given a limited size dataset, for example the sequential approach of building a model based upon currently available data and testing on data from new patients when they become available, or withholding an arbitrary selection of subjects from the modeling as a test set and testing the model on these subjects. Internal validation approaches such as cross-validation or related bootstrapping methods may also be useful to assess the model selection *procedure*, but tend to overestimate the performance of a specific predictive model in subsequent external validation.[80,81] The key properties to consider when selecting an assessment method are to ensure that it will provide both precise and unbiased information regarding the prediction error rate of the potential model to be tested for clinical use. As well as assessing an overall predictive rate, it is also useful to separately assess the predictive rate for both the cases and controls and to consider the relative costs of making these false predictions within a clinical setting. Finally, the prevalence of the condition in question (here ILD) is also a critical factor in estimating what proportion of people predicted to be at risk are truly at risk, and this should also be borne in mind when evaluating a model for potential clinical use. The recently published FDA concept paper on drug-diagnostic co-

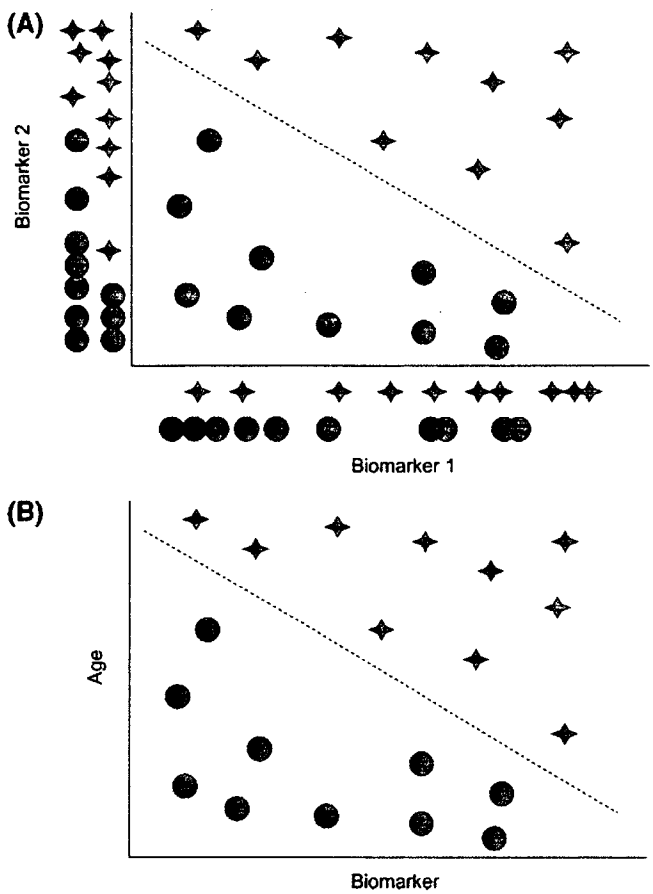

Figure 7. (A) Hypothetical example of the combined disease-linkage effect of two protein biomarkers. (Stars signify affected case individuals, circles non-affected control individuals). (B) Hypothetical example of the combined disease-linkage effect of a biomarker and a clinical variable. (Stars signify affected case individuals, circles non-affected control individuals).

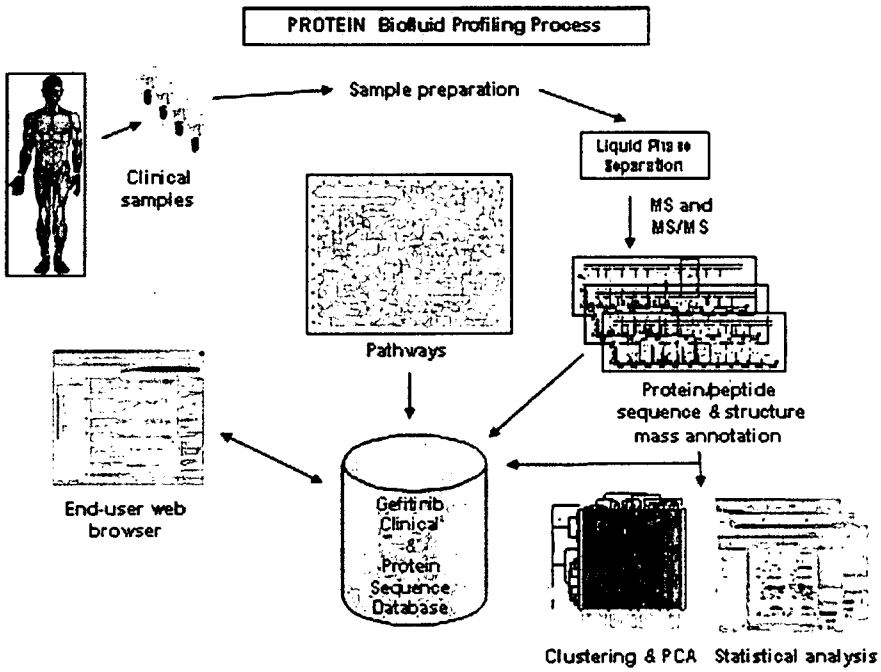

Figure 8. Illustration of the bioinformatics and data processing structure within which MSBA (Mass Spectrometric Biomarker Assays) data are captured, modified and analyzed.

development discusses many of the issues around validating predictive biomarkers.[82]

Finally, it is preferable to be able to assign a biological rationale to the biomarkers. Confidence in the reliability of a biomarker is greatly enhanced if we can correctly understand how it relates to the mechanism and progression of the disease of interest. Figure 8 illustrates a bioinformatics and data processing structure that we have developed to allow us to both conduct interactive exploratory and statistical analyses, and also investigate the disease and pathway linkage of discovered biomarker proteins through direct access to reference databases.

Future Perspectives

Within this paper we have discussed many of the issues that need to considered in developing a personalized medicine approach. A key starting point is that rigorous steps are taken to ensure accurate diagnosis and the careful gathering of both clinical and proteomic data to facilitate the search for peptide patterns.

There are many challenges in performing protein analysis in blood, but mass spectrometry equipment and methods can now be used to generate peptide data with high sensitivity, high scanning speed, and improved quantification. Data handling and processing techniques for steps such as peak alignment and the subsequent methodologies for statistical modeling and analysis are now far enough developed to generate high quality data and robustly analyze these data with confidence.

We have provided details of the MSBA method that can be used to easily translate protein intensities into a practical multiplex assay which can be exploited in the clinic without the need to develop anti-bodies for ELISA. We have also described how an expanded statistical analysis can be used to allow for the individual variance of protein expression to enable us to focus on the proteomic patterns that are actually related to ILD. Finally, we have emphasized the importance of validating the predictive power of a biomarker tool in a way that reflects the real-life setting of intended clinical use.

Hopefully, this combination of developments over a range of different areas brings us one step closer to a practical personalized medicine.

IRESSA is a trademark of the AstraZeneca group of companies.

Acknowledgments. We thank all involved in the Iressa study which provided the inspiration for this overview of personalized medicine approaches, including: the external Epidemiology Advisory Board (Kenneth J. Rothman, Jonathan M. Samet, Toshiro Takezaki, Kotaro Ozasa, Masahiko Ando) for their advice and scientific review of study design, conduct, and analysis; Professor Nestor Müller for his expert input into radiological aspects of ILD diagnosis; all Case Review Board members individually (M. Suga, T. Johkoh, M. Takahashi, Y. Ohno, S. Nagai, Y. Taguchi, Y. Inoue, T. Yana, M. Kusumoto, H. Arakawa, A. Yoshimura, M. Nishio, Y. Ohe, K. Yoshimura, H. Takahashi, Y. Sugiyama, M. Ebina) for their valuable work in blindly reviewing ILD diagnoses, as well as pre-study CT scans for pre-existing comorbidities, the Japan Thoracic Radiology Group, Shiga, Japan for their support of CRB work; and all Hospitals, Clinical Investigators, study monitors, nurses, data managers, other support staff, and the participating patients for providing and collecting the data in the study.

References

(1) Thatcher, N.; Chang, A.; Parikh, P.; Pereira, J. R.; Ciuleanu, T.; von Pawel, J.; et al. Gefitinib plus best supportive care in previously treated patients with refractory advanced non-small-cell lung cancer: results from a randomised, placebo-controlled, multicentre study (Iressa Survival Evaluation in Lung Cancer). *Lancet* **2005**, *366*, 1527–1537.

(2) Hirsch, F. R.; Varella-Garcia, M.; McCoy, J.; West, H.; Xavier, A. C.; Gumerlock, P.; et al. Increased epidermal growth factor receptor gene copy number detected by fluorescence in situ hybridization associates with increased sensitivity to gefitinib in patients with bronchioloalveolar carcinoma subtypes: a Southwest Oncology Group study. *J. Clin. Oncol.* **2005**, *23*, 6838–6845.

(3) Cappuzzo, F.; Varella-Garcia, M.; Shigematsu, H.; Domenichini, I.; Bartolini, S.; Ceresoli, G. L.; et al. Increased HER2 gene copy number is associated with response to gefitinib therapy in epidermal growth factor receptor-positive non-small-cell lung cancer patients. *J. Clin. Oncol.* **2005**, *23*, 5007−5018.
(4) Araki, J.; Okamoto, I.; Suto, R.; Ichikawa, Y.; Sasaki, J. Efficacy of the tyrosine kinase inhibitor gefitinib in a patient with metastatic small cell lung cancer. *Lung Cancer* **2005**, *48*, 141−144.
(5) Kim, K. S.; Jeong, J. Y.; Kim, Y. C.; Na, K. J.; Kim, Y. H.; Ahn, S. J.; et al. Predictors of the response to gefitinib in refractory non-small cell lung cancer. *Clin. Cancer Res.* **2005**, *11*, 2244−2251.
(6) Lynch, T. J.; Bell, D. W.; Sordella, R.; Gurubhagavatula, S.; Okimoto, R. A.; Brannigan, B. W.; et al. Activating mutations in the epidermal growth factor receptor underlying responsiveness of non-small-cell lung cancer to gefitinib. *N. Engl. J. Med.* **2004**, *350*, 2129−2139.
(7) Paez, J. G.; Jänne, P. A.; Lee, J. C.; Tracy, S.; Greulich, H.; Gabriel, S.; et al. EGFR mutations in lung cancer: correlation with clinical response to gefitinib therapy. *Science* **2004**, *304*, 1497−1500.
(8) Shigematsu, H.; Lin, L.; Takahashi, T.; Nomura, M.; Suzuki, M.; Wistuba II; et al. Clinical and biological features associated with epidermal growth factor receptor gene mutations in lung cancers. *J. Natl. Cancer Inst.* **2005**, *97*, 339−346.
(9) American Thoracic Society: American Thoracic Society/European Respiratory Society International Multidisciplinary Consensus Classification of the Idiopathic Interstitial Pneumonias. This joint statement of the American Thoracic Society (ATS), and the European Respiratory Society (ERS) was adopted by the ATS Board of Directors, June 2001 and by The ERS Executive Committee, June 2001. *Am. J. Respir. Crit. Care Med.* **2002**, *165*, 277−304.
(10) Raghu, G.; Nyberg, F.; Morgan, G. The epidemiology of interstitial lung disease and its association with lung cancer. *Br. J. Cancer* **2004**, *91* (Suppl. 2), S3−S10.
(11) Asada, K.; Mukai, J.; Ougushi, F. Characteristics and management of lung cancer in patients with idiopathic pneumonia. *Jap. J. Thor. Dis.* **1992**, *51*, 214−219.
(12) Hubbard, R.; Venn, A.; Lewis, S.; Britton, J. Lung cancer and cryptogenic fibrosing alveolitis. A population-based cohort study. *Am. J. Respir. Crit. Care Med.* **2000**, *161*, 5−8.
(13) Matsushita, H.; Tanaka, S.; Saiki, Y.; Hara, M.; Nakata, K.; Tanimura, S.; et al. Lung cancer associated with usual interstitial pneumonia. *Pathol. Int.* **1995**, *45*, 925−932.
(14) Ogura, T.; Kondo, A.; Sato, A.; Ando, M.; Tamura, M. Incidence and clinical features of lung cancer in patients with idiopathic interstitial pneumonia. *Nihon Kyobu Shikkan Gakkai Zasshi* **1997**, *35*, 294−299.
(15) Takeuchi, E.; Yamaguchi, T.; Mori, M.; Tanaka, S.; Nakagawa, M.; Yokota, S.; et al. Characteristics and management of patients with lung cancer and idiopathic interstitial pneumonia. *Nihon Kyobu Shikkan Gakkai Zasshi* **1996**, *34*, 653−658.
(16) Turner-Warwick, M.; Lebowitz, M.; Burrows, B.; Johnson, A. Cryptogenic fibrosing alveolitis and lung cancer. *Thorax* **1980**, *35*, 496−499.
(17) Baumgartner, K. B.; Samet, J. M.; Stidley, C. A.; Colby, T. V.; Waldron, J. A. Cigarette smoking: a risk factor for idiopathic pulmonary fibrosis. *Am. J. Respir. Crit. Care Med.* **1997**, *155*, 242−248.
(18) Britton, J.; Hubbard, R. Recent advances in the aetiology of cryptogenic fibrosing alveolitis. *Histopathology* **2000**, *37*, 387−392.
(19) Iwai, K.; Mori, T.; Yamada, N.; Yamaguchi, M.; Hosoda, Y. Idiopathic pulmonary fibrosis. Epidemiologic approaches to occupational exposure. *Am. J. Respir. Crit. Care Med.* **1994**, *150*, 670−675.
(20) Nagai, S.; Hoshino, Y.; Hayashi, M.; Ito, I. Smoking-related interstitial lung diseases. *Curr. Opin. Pulm. Med.* **2000**, *6*, 415−419.
(21) Lilly. Gemcitabine prescribing information. http://pi.lilly.com/gemzar.pdf, 2003.
(22) Kunitoh, H.; Watanabe, K.; Onoshi, T.; Furuse, K.; Niitani, H.; Taguchi, T. Phase II trial of docetaxel in previously untreated advanced non-small-cell lung cancer: a Japanese cooperative study. *J. Clin. Oncol.* **1996**, *14*, 1649−1655.
(23) Merad, M.; Le Cesne, A.; Baldeyrou, P.; Mesurolle, B.; Le Chevalier, T. Docetaxel and interstitial pulmonary injury. *Ann. Oncol.* **1997**, *8*, 191−194.
(24) Wang, G.-S.; Yan, K.-Y.; Perng, R.-P. Life-threatening hypersensitivity pneumonitis induced by docetaxel (taxotere). *Br. J. Cancer* **2001**, *85*, 1247−1250.
(25) Erasmus, J. J.; McAdams, H. P.; Rossi, S. E. Drug-induced lung injury. *Semin. Roentgenol.* **2002**, *37*, 72−81.
(26) Aviram, G.; Yu, E.; Tai, P.; Lefcoe, M. S. Computed tomography to assess pulmonary injury associated with concurrent chemoradiotherapy for inoperable non-small cell lung cancer. *Can. Assoc. Radiol. J.* **2001**, *52*, 385−391.
(27) Yoshida, S. The results of gefitinib prospective investigation. *Med. Drug J.* **2005**, *41*, 772−789.
(28) Mueller, N. L.; White, D. A.; Jiang, H.; Gemma, A. Diagnosis and management of drug-associated interstitial lung disease. *Br. J. Cancer* **2004**, *91*, S24−S30.
(29) Marko-Varga, G.; Fehniger, T. E. Proteomics and disease—the challenges for technology and discovery. *J. Proteome Res.* **2004**, *3*, 167−178.
(30) Marko-Varga, G.; Lindberg, H.; Lofdahl, C. G.; Jonsson, P. H. L.; Dahlback, M.; Lindquist, E.; et al. Discovery of biomarker candidates within disease by protein profiling: principles and concepts. *J. Proteome Res.* **2005**, *4*, 1200−1212.
(31) Omenn, G. S. The Human Proteome Organization Plasma Proteome Project pilot phase: reference specimens, technology platform comparisons, and standardized data submissions and analyses. *Proteomics* **2004**, *4*, 1235−1240.
(32) Omenn, G. S. Advancement of biomarker discovery and validation through the HUPO plasma proteome project. *Dis. Markers* **2004**, *20*, 131−134.
(33) Orchard, S.; Hermjakob, H.; Binz, P. A.; Hoogland, C.; Taylor, C. F.; Zhu, W.; et al. Further steps towards data standardisation: the Proteomic Standards Initiative HUPO 3(rd) annual congress, Beijing 25−27(th) October, 2004. *Proteomics* **2005**, *5*, 337−339.
(34) Anderson, N. G.; Matheson, A.; Anderson, N. L. Back to the future: the human protein index (HPI) and the agenda for post-proteomic biology. *Proteomics* **2001**, *1*, 3−12.
(35) Anderson, N. L.; Anderson, N. G. The human plasma proteome: history, character, and diagnostic prospects. *Mol. Cell. Proteomics* **2002**, *1*, 845−867.
(36) Jacobs, J. M.; Adkins, J. N.; Qian, W. J.; Liu, T.; Shen, Y.; Camp, D. G.; et al. Utilizing human blood plasma for proteomic biomarker discovery. *J. Proteome Res.* **2005**, *4*, 1073−1085.
(37) Anderson, N. G.; Anderson, L. The Human Protein Index. *Clin. Chem.* **1982**, *28*, 739−748.
(38) Haab, B. B.; Geierstanger, B. H.; Michailidis, G.; Vitzthum, F.; Forrester, S.; Okon, R.; et al. Immunoassay and antibody microarray analysis of the HUPO Plasma Proteome Project reference specimens: systematic variation between sample types and calibration of mass spectrometry data. *Proteomics* **2005**, *5*, 3278−3291.
(39) Martens, L.; Hermjakob, H.; Jones, P.; Adamski, M.; Taylor, C.; States, D.; et al. PRIDE: the proteomics identifications database. *Proteomics* **2005**, *5*, 3537−3545.
(40) Omenn, G. S.; States, D. J.; Adamski, M.; Blackwell, T. W.; Menon, R.; Hermjakob, H.; et al. Overview of the HUPO Plasma Proteome Project: results from the pilot phase with 35 collaborating laboratories and multiple analytical groups, generating a core dataset of 3020 proteins and a publicly-available database. *Proteomics* **2005**, *5*, 3226−3245.
(41) Patterson, S. D. Data analysis—the Achilles heel of proteomics. *Nat. Biotechnol.* **2003**, *21*, 221−222.
(42) Rahbar, A. M.; Fenselau, C. Integration of Jacobson's pellicle method into proteomic strategies for plasma membrane proteins. *J. Proteome Res.* **2004**, *3*, 1267−1277.
(43) Ho, Y.; Gruhler, A., Heilbut, A.; Bader, G. D.; Moore, L.; Adams, S. L.; et al. Systematic identification of protein complexes in Saccharomyces cerevisiae by mass spectrometry. *Nature* **2002**, *415*, 180−183.
(44) Aebersold, R.; Mann, M. Mass spectrometry-based proteomics. *Nature* **2003**, *422*, 198−207.
(45) Anderson, N. L.; Polanski, M.; Pieper, R.; Gatlin, T.; Tirumalai, R. S.; Conrads, T. P.; et al. The human plasma proteome: a nonredundant list developed by combination of four separate sources. *Mol. Cell. Proteomics* **2004**, *3*, 311−326.
(46) Olsen, J. V.; Mann, M. Improved peptide identification in proteomics by two consecutive stages of mass spectrometric fragmentation. *Proc. Natl. Acad. Sci. U.S.A.* **2004**, *101*, 13417−13422.
(47) Sadygov, R. G.; Liu, H.; Yates, J. R. Statistical models for protein validation using tandem mass spectral data and protein amino acid sequence databases. *Anal. Chem.* **2004**, *76*, 1664−1671.
(48) Fujii, K.; Nakano, T.; Kanazawa, M.; Akimoto, S.; Hirano, T.; Kato, H.; et al. Clinical-scale high-throughput human plasma proteome analysis: lung adenocarcinoma. *Proteomics* **2005**, *5*, 1150−1159.

(49) Campbell, J. M.; Collings, B. A.; Douglas, D. J. A new linear ion trap time-of-flight system with tandem mass spectrometry capabilities. *Rapid Commun. Mass Spectrom.* **1998**, *12*, 1463–1474.
(50) Cha, B. C.; Blades, M.; Douglas, D. J. An interface with a linear quadropole ion guide for an electrospray-ion trap mass spectrometer system. *Anal. Chem.* **2000**, *72*, 5647–5654.
(51) Hager, J. W. Product ion spectral simplification using time-delayed fragment ion capture with tandem linear ion traps. *Rapid Commun. Mass Spectrom.* **2003**, *17*, 1389–1398.
(52) Syka, J. E.; Marto, J. A.; Bai, D. L.; Horning, S.; Senko, M. W.; Schwartz, J. C.; et al. Novel linear quadrupole ion trap/FT mass spectrometer: performance characterization and use in the comparative analysis of histone H3 post-translational modifications. *J. Proteome Res.* **2004**, *3*, 621–626.
(53) Shen, Y.; Zhao, R.; Belov, M. E.; Conrads, T. P.; Anderson, G. A.; Tang, K.; et al. Packed capillary reversed-phase liquid chromatography with high-performance electrospray ionization Fourier transform ion cyclotron resonance mass spectrometry for proteomics. *Anal. Chem.* **2001**, *73*, 1766–1775.
(54) Wu, S. L.; Kim, J.; Hancock, W. S.; Karger, B. Extended Range Proteomic Analysis (ERPA): a new and sensitive LC-MS platform for high sequence coverage of complex proteins with extensive post-translational modifications-comprehensive analysis of beta-casein and epidermal growth factor receptor (EGFR). *J. Proteome Res.* **2005**, *4*, 1155–1170.
(55) Olsen, J. V.; de Godoy, L. M.; Li, G.; Macek, B.; Mortensen, P.; Pesch, R.; et al. Parts per million mass accuracy on an Orbitrap mass spectrometer via lock mass injection into a C-trap. *Mol. Cell. Proteomics* **2005**, *4*, 2010–2021.
(56) Yates, J. R.; Cociorva, D.; Liao, L.; Zabrouskov, V. Performance of a linear ion trap-Orbitrap hybrid for peptide analysis. *Anal. Chem.* **2006**, *78*, 493–500.
(57) Anderson, D. C.; Li, W.; Payan, D. G.; Noble, W. S. A new algorithm for the evaluation of shotgun peptide sequencing in proteomics: support vector machine classification of peptide MS/MS spectra and SEQUEST scores. *J. Proteome Res.* **2003**, *2*, 137–146.
(58) Carr, S.; Aebersold, R.; Baldwin, M.; Burlingame, A.; Clauser, K.; Nesvizhskil, A. The need for guidelines in publication of peptide and protein identification data: working group on publication guidelines for peptide and protein identification data. *Mol. Cell. Proteomics* **2004**, *3*, 531–533.
(59) Fenyo, D.; Beavis, R. C. A method for assessing the statistical significance of mass spectrometry-based protein identifications using general scoring schemes. *Anal. Chem.* **2003**, *75*, 768–774.
(60) Nesvizhskii, A. I.; Keller, A.; Kolker, E.; Aebersold, R. A statistical model for identifying proteins by tandem mass spectrometry. *Anal. Chem.* **2003**, *75*, 4646–4658.
(61) Peri, S.; Navarro, J. D.; Kristiansen, T. Z.; Amanchy, R.; Surendranath, V.; Muthusamy, B.; et al. Human protein reference database as a discovery resource for proteomics. *Nucleic Acids Res.* **2004**, *32*, D497–D501.
(62) Kratchmarova, I.; Blagoev, B.; Haack-Sorensen, M.; Kassem, M.; Mann, M. Mechanism of divergent growth factor effects in mesenchymal stem cell differentiation. *Science* **2005**, *308*, 1472–1477.
(63) Dreger, M.; Bengtsson, L.; Schöneberg, T.; Otto, H.; Hucho, F. Nuclear envelope proteomics: novel integral membrane proteins of the inner nuclear membrane. *Proc. Natl. Acad. Sci. U.S.A.* **2001**, *98*, 11943–11948.
(64) Giot, L.; Bader, J. S.; Brouwer, C.; Chaudhuri, A.; Kuang, B.; Li, Y.; et al. A protein interaction map of Drosophilia melanogaster. *Science* **2003**, *302*, 1727–1736.
(65) Johnson, J. R.; Florens, L.; Carucci, D. J.; Yates, J. R., III. Proteomics in malaria. *J. Proteome Res.* **2004**, *3*, 296–306.
(66) Hirsch, J.; Hansen, K. C.; Burlingame, A. L.; Matthay, M. A. Proteomics: current techniques and potential applications to lung disease. *Am. J. Physiol. Lung Cell Mol. Physiol.* **2004**, *287*, L1–L23.
(67) Malmström, J.; Larsen, K.; Hansson, L.; Löfdahl, C.-G.; Norregard-Jensen, O.; Marko-Varga, G.; et al. Proteoglycan and proteome profiling of central human pulmonary fibrotic tissue utilizing minaturized sample preparation: A feasibility study. *Proteomics* **2002**, *2*, 394–404.
(68) Malmström, J.; Larsen, K.; Malmström, L.; Tufvesson, E.; Parker, K.; Marchese, J.; et al. Proteome annotations and identifications of the human pulmonary fibroblast. *J. Proteome Res.* **2004**, *3*, 525–537.
(69) Oh, P.; Li, Y.; Yu, J.; Durr, E.; Krasinska, K. M.; Carver, L. A.; et al. Subtractive proteomic mapping of the endothelial surface in lung and solid tumours for tissue-specific therapy. *Nature* **2004**, *429*, 629–635.
(70) Fujii, K.; Nakano, T.; Kawamura, T.; Usui, F.; Bando, Y.; Wang, R.; et al. Multidimensional protein profiling technology and its application to human plasma proteome. *J. Proteome Res.* **2004**, *3*, 712–718.
(71) Schwartz, J. C.; Senko, M. W.; Syka, J. E. A two-dimensional quadrupole ion trap mass spectrometer. *J. Am. Soc. Mass Spectrom.* **2002**, *13*, 659–669.
(72) Sneath, P. H. A.; Sokai, R. R. *Numerical Taxonomy, The principles and practice of numerical classification*; W. H. Freeman and Co.: San Francisco, 1973.
(73) Smith, C. A.; Want, E. J.; O'Maille, G.; Abagyan, R.; Siuzdak, G. XCMS: processing mass spectrometry data for metabolite profiling using nonlinear peak alignment, matching, and identification. *Anal. Chem.* **2006**, *78*, 779–787.
(74) Perkins, D. N.; Pappin, D. J.; Creasy, D. M.; Cottrell, J. S. Probability-based protein identification by searching sequence-databases using mass spectrometry data. *Electrophoresis* **1999**, *20*, 3551–3567.
(75) Storey, J. A direct approach to false discovery rates. *J. R. Stat. Soc. Ser. B* **2002**, *64*, 479.
(76) Vapnik, V. *Statistical Learning Theory*; Wiley: Chichester, UK, 1998.
(77) Breiman, L. Random forests. *Mach. Learn.* **2001**, *45*, 5–32.
(78) Tibshirani, R.; Hastie, T.; Narasimhan, B.; Chu, G. Diagnosis of multiple cancer types by shrunken centroids of gene expression. *Proc. Natl. Acad. Sci. U.S.A.* **2002**, *99*, 6567–6572.
(79) Lee, J. W.; Lee, J. B.; Park, M.; Song, S. H. An extensive comparison of recent classification tools applied to microarray data. *Comp. Stat. Data Anal.* **2005**, *48*, 869–885.
(80) Steyerberg, E. W.; Harrell, F. E., Jr.; Borsboom, G. J.; Eijkemans, M. J.; Vergouwe, Y.; Habbema, J. D. Internal validation of predictive models: efficiency of some procedures for logistic regression analysis. *J. Clin. Epidemiol.* **2001**, *54*, 774–781.
(81) Bleeker, S. E.; Moll, H. A.; Steyerberg, E. W.; Donders, A. R.; Derksen-Lubsen, G.; Grobbee, D. E.; et al. External validation is necessary in prediction research: a clinical example. *J. Clin. Epidemiol.* **2003**, *56*, 826–832.
(82) Food and Drug Administration (FDA): Drug-diagnostic co-development concept paper. Draft—not for implementation. http://www.fda.gov/cder/genomics/pharmacoconceptfn.pdf, 2005.

PR070046S

Lung Cancer (2007) 57, 302–310

available at www.sciencedirect.com

ScienceDirect

journal homepage: www.elsevier.com/locate/lungcan

LUNG CANCER

Abrogation of the interaction between osteopontin and αvβ3 integrin reduces tumor growth of human lung cancer cells in mice

Ri Cui[a,b,*], Fumiyuki Takahashi[a,b], Rina Ohashi[a,b], Tao Gu[a,b], Masakata Yoshioka[a,b], Kazuto Nishio[c], Yuichiro Ohe[d], Shigeru Tominaga[a], Yumiko Takagi[a,b], Shinichi Sasaki[a], Yoshinosuke Fukuchi[a,b], Kazuhisa Takahashi[a,b]

[a] *Department of Respiratory Medicine and Research Institute for Diseases of Old Ages, Juntendo University, School of Medicine, 2-1-1 Hongo, Bunkyo-Ku, Tokyo 113-8421, Japan*
[b] *Research Institute for Diseases of Old Ages, Juntendo University, School of Medicine, 2-1-1 Hongo, Bunkyo-Ku, Tokyo 113-8421, Japan*
[c] *Pharmacology Division, National Cancer Center Research Institute, 5-1-1 Tsukiji, Chuo-Ku, Tokyo 104-0045, Japan*
[d] *Department of Internal Medicine, National Cancer Center Hospital, 5-1-1 Tsukiji, Chuo-Ku, Tokyo 104-0045, Japan*

Received 4 January 2007; received in revised form 15 March 2007; accepted 18 March 2007

KEYWORDS
Osteopontin;
Angiogenesis;
αvβ3 integrin;
Tumor growth;
Lung cancer

Summary Osteopontin (OPN) is a multifunctional cytokine involved in cell signaling by interacting with αvβ3 integrins. Recent clinical studies have indicated that OPN expression is associated with tumor progression and poor prognosis among patients with lung cancer. However, the biological role of OPN in human lung cancer has not yet been well-defined. The purpose of this study is to investigate and provide evidence for the causal role of OPN regarding tumor growth and angiogenesis in human lung cancer. In this study, we developed a stable OPN transfectant from human lung cancer cell line SBC-3 which does not express the intrinsic OPN mRNA. To reveal the in vivo effect of OPN on tumor growth of human lung cancer, we subcutaneously injected OPN-overexpressing SBC-3 cells (SBC-3/OPN) and control cells (SBC-3/NEO) into the nude mice. Transfection with the OPN gene significantly increased in vivo tumor growth and neovascularization of SBC-3 cells in mice. These in vivo effects of OPN were markedly suppressed with administration of anti-αvβ3 integrin monoclonal antibody or anti-angiogenic agent, TNP-470. Furthermore, recombinant OPN protein enhanced human umbilical vein endothelial cell (HUVEC) proliferation in vitro, and this enhancement was significantly inhibited with the

* Corresponding author at: Department of Respiratory Medicine, Juntendo University, School of Medicine, 2-1-1 Hongo, Bunkyo-Ku, Tokyo 113-8421, Japan. Tel.: +81 3 5802 1063; fax: +81 3 5802 1617.
E-mail address: cri@med.juntendo.ac.jp (R. Cui).

0169-5002/$ – see front matter
doi:10.1016/j.lungcan.2007.03.019

addition of anti-αvβ3 integrin antibody. Taken together, these results suggest that OPN plays a crucial role for tumor growth and angiogenesis of human lung cancer cells in vivo by interacting with αvβ3 integrin. Targeting the interaction between OPN and αvβ3 integrin could be effective for future development of anti-angiogenic therapeutic agents for patients with lung cancer.

1. Introduction

Lung cancer is one of the most frequently diagnosed solid tumors in the world, and is the leading cause of cancer-related deaths in Japan [1]. Despite advancement and improvements in surgical and medical treatments, the prognosis of lung cancer patients remains extremely poor [2]. These facts indicate how important it is to identify novel target molecules for the development of new anticancer therapies for human lung cancer.

Tumor growth and metastasis depend on blood supply and vessel formation. Therefore, anti-angiogenic therapy appears to be an attractive and rational approach for the treatment of solid tumors including lung cancer [3,4]. One approach to anti-angiogenic therapy is to inhibit the adhesive interactions required for tumor angiogenesis. The migration and proliferation of vascular endothelial cells is dependent on their adhesiveness to extracellular matrix (ECM) proteins through a variety of cell adhesion receptor including αvβ3 integrin [5,6]. Thus, the interaction between ECM and αvβ3 integrin may be a therapeutic target for lung cancer patients.

Osteopontin (OPN) is a multifunctional phosphoprotein that binds to αv integrin at the arginine-glycine-asparatic acid (RGD) motif of the central portion and exerts cell-adhesion and migration activity [7,8]. OPN is one of the ECM proteins produced by cancer cells, and is revealed to be overexpressed in various human tumors including the lung, breast, colon, ovary, and gastric cancers [9–14]. Previous studies suggested that OPN may be involved in the angiogenesis of cancer cells. For example, Senger et al. reported that OPN promotes vascular endothelial cell migration via αv integrin in cooperation with vascular endothelial growth factor (VEGF), suggesting that OPN may be involved in angiogenesis [15]. Shijubo et al. demonstrated that coexpression of OPN and VEGF is closely associated with angiogenesis and poor prognosis in stage I lung adenocarcinoma [16]. Thus, OPN is postulated to be related with tumor progression and angiogenesis in various cancers.

Recently, much interest has been focused on OPN expression in human lung cancer. Donati et al. investigated on the correlation between OPN expression in tumor tissues and survival of 136 patients with stage I non-small cell lung cancer (NSCLC), and indicated that OPN expression is a significant unfavorable prognostic factor for survival among patients with stage I NSCLC [17]. Hu et al. also reported that OPN expression was associated with tumor growth, tumor staging, and lymph node invasion of patients with NSCLC. They further analyzed OPN levels in plasma, and suggest that plasma OPN levels may serve as a biomarker for diagnosing or monitoring patients with NSCLC [18]. These findings from these clinical studies imply that OPN may be a therapeutic target and useful biomarker for human lung cancer. However, the biological and functional role of OPN in lung cancer animal model and therapeutic trials targeting OPN and its receptor, αvβ3 integrin, have not yet been reported.

In this study, we first developed stable transfectants from human small cell lung cancer (SCLC) cell line SBC-3 that constitutively secrete mouse OPN. We demonstrated that OPN transfected SBC-3 cells significantly increased in vivo tumorigenecity and neovascularization in comparison with the control cells in mice. In addition, we evaluated the therapeutic efficacy of anti-mouse αvβ3 integrin antibody (RMV-7) against OPN-overexpressing SBC-3 cells inoculated mice. The biological significance of OPN in tumor growth and angiogenesis of lung cancer and potential treatment using RMV-7 antibody are also discussed.

2. Materials and methods

2.1. Cell lines and reagents

Human small cell lung cancer cell line, SBC-3 cells, was kindly provided by Dr. I. Kimura (Okayama University, Okayama), and cultured in RPMI1640 (Koujin Bio, Saitama, Japan) medium containing 10% (v/v) fetal calf serum. HUVEC were purchased from Clonetics (San Diego, CA) and maintained with EGM-2 medium (Clonetics) on collagen-coated plastic flasks. The anti-mouse αvβ3 antibody (RMV-7) was kindly provided by Prof. Okumura (Department of Immunology, Juntendo University), and has been proven to interfere with OPN-mediated cell migration, adhesion, and proliferation [19,20]. Anti-human αvβ3 monoclonal antibody (LM609) was purchased from Chemicon International (Australia). The monoclonal antibody against murine CD31 was purchased from Pharmingen (San Diego, CA). The monoclonal antibody against murine OPN was purchased from Immuno-Biological Laboratories (Gunma, Japan). The polyclonal rabbit anti-single stranded DNA (ssDNA) was purchased from Dakocytomation (Tokyo, Japan). TNP-470 (6-*O*-(*N*-chloroacethyl-carbamoyl)-fumagillol), a semisynthetic analog of fumagillin derived from *Aspergillus fumigatus*, was kindly provided by Takeda Chemical Industries (Osaka, Japan).

2.2. Transfection

5×10^5 SBC-3 cells were transfected with Lipofectamine Reagent (Invitrogen) using 8 μg of purified murine OPN cDNA cloned into the eukaryotic cDNA expression vector BMGneo as previously described [21]. This plasmid was designated as BMGneo-mOPN. Two days later, the cells were placed in G418 sulfate (Geneticin; Invitrogen) at 1 mg/ml for selection. Four weeks after transfection, G418-resistant colonies were expanded and isolated with limiting dilution. The

resulting selected and isolated SBC-3 cells transfected with BMGneo-mOPN and BMGneo were designated as SBC-3/OPN and SBC-3/NEO, respectively.

2.3. Detection of OPN and VEGF transcription by RT-PCR

Expression of OPN and VEGF mRNA were assessed by RT-PCR. Total RNAs were extracted from cultured cell lines with TRIzol reagent (Invitrogen). The primers for the RT-PCR were: OPN sense primer (5′-AGTCGACATGAGATTGGCAGTGATTTGC-3′), OPN anti-sense primer (5′-ACTCGAGGCCTCTTCTTTAGTTGACCTC-3′), VEGF sense primer (5′-TGCACCCATGGCAGAAGGAGG-3′), and VEGF anti-sense primer (5′-TCACCGCCTCGGCTTGTCACA-3′). RT-PCR was conducted using a Gene Amp RNA PCR kit (Applied Biosystems, Branchburg, NJ) according to the manufacture's instructions.

2.4. Determination of OPN protein secretion by ELISA

5×10^5 SBC-3/OPN transfectants were cultured in 6-well plates with 2% FCS in RPMI 1640 medium overnight, followed by incubation in 3 ml serum free medium for an additional 24 h. Secreted murine OPN protein level in culture supernatant was measured with the commercial ELISA kit (Immuno-Biological Laboratories, Gunma, Japan) according to the manufacturer's instruction.

2.5. Western blot analysis

Conditioned medium from SBC-3/OPN and SBC-3/NEO cells were subjected to western blot analysis. Samples were separated on 10% acrylamide gels and transferred to a nitrocellulose filter with electroblotting at 4 °C. The filters were blocked in phosphate-buffered saline (PBS) containing 10% dry milk, washed in PBS containing 1% dry milk and 0.5% Tween-20, and then incubated with polyclonal rabbit anti-mouse OPN antibody (Immuno-Biological Laboratories, Gunma, Japan) at room temperature for 1 h. Filters were again washed and then incubated with horseradish-peroxidase-conjugated anti-rabbit antibody (Amersham Pharmacia Biotech) for 1 h. Filters were then washed with TBST (150 mM NaCl, 10 mM Tris, pH 8.0, 0.05% Tween-20), and specific proteins were detected using the enhanced chemiluminescence system (Amersham Pharmacia Biotech).

2.6. In vitro cell growth rates

SBC-3/NEO and SBC-3/OPN were placed onto 96-well plates at 2×10^3 cells/well in triplicate. At designated time points, the number of cells were quantified using a colormetric MTT assay as described previously [22].

2.7. In vitro cell migration assay

SBC-3/OPN and SBC-3/NEO were transfered to 6-well culture plates at 5×10^5 cells/well and incubated with 2% FCS in RPMI 1640 medium overnight. The cells were washed in PBS, and 3 ml of serum free medium were added to each well. After 24 h, 3 ml of conditioned serum-free medium were collected and subjected to in vitro cell migration assay. In vitro cell migration was performed using a cell culture insert with 8 μm micropore membrane (Falcon; Becton Dickinson, Franklin Lake, NJ) as previously described [21]. Briefly, the suspension of HUVEC (5×10^4 cells/200 μl in RPMI 1640 containing 0.1% BSA) was added to the upper chamber and the collected medium was added to the lower chamber. In order to confirm cell migration mediated by OPN, we conducted additional experiments by treating the cells with GRGDS peptide (Sigma) at the concentration of 100 μM or anti-human αvβ3 antibody at the concentration of 10 μg/ml. After incubation at 37 °C for 8 h, the filters were fixed with 10% formalin, and stained with crystal violet. The cells on the upper surface of the filters were removed by swabbing with a cotton swab, and the cells that had migrated to the lower surface were counted under a microscope at the magnification of 200×. All assays were performed in triplicate and at least three independent experiments were performed.

2.8. Soft agar colony formation assay

Six-well culture plates were covered with a layer of 0.5% agar in RPMI 1640 medium containing 20% (v/v) fetal calf serum to prevent the attachment of the cells to plastic substratum. Cell suspensions (5×10^3 cells/well) of the SBC-3/OPN or SBC-3/NEO cells were prepared with 0.3% agar and poured into 6-well plates. After 2 weeks of incubation at 37 °C, the colonies containing at least 50 cells were counted. All assays were performed in triplicate.

2.9. Mice

Female athymic BALB/c nude mice, 6—7 weeks old, were purchased from Charlsriver Co., Ltd. (Tokyo, Japan) and maintained in our animal facilities under specific pathogen-free conditions. All animal experiments were performed according to the Guidelines on Animal Experimentation as established by Juntendo University, School of Medicine.

2.10. In vivo tumorigenicity

SBC-3/OPN and SBC-3/NEO cells were harvested from the culture flask with 0.05% Trypsin-EDTA (Invitrogen), washed three times, resuspended in PBS. Cell viability was determined by trypan blue dye exclusion test and cells were inoculated subcutaneously (s.c.) into the left flank of nude mice (1×10^7 cells/mouse). To investigate whether tumor growth is mediated by the interaction between OPN and its receptor, the RMV-7 antibody was administered to SBC-3/OPN or SBC-3/NEO inoculated mice. Briefly, RMV-7 (200 μg/mouse) and control isotype-matched IgG (200 μg/mouse) were administered intraperitoneally from day 3 after inoculation three times a week for 3 weeks. TNP-470 (30 mg/kg) was also administered subcutaneously from day 7 twice a week for 3 weeks to reveal the involvement of angiogenesis in in vivo tumor growth. Tumor growth was measured with a digital caliper in two perpendicular diameters every week. Tumor volumes were calculated from the length (a) and width (b) by using the following formula:

volume (mm^3) = $ab^2/2$. Each group consisted of 10 mice. All experiments were performed twice.

2.11. Immunohistochemical staining

Histological sections were obtained from SBC-3/OPN and SBC-3/NEO tumor tissues resected from mice. After resection, tumor tissues were immediately embedded and frozen in Tissue-Tek OCD compound (Miles Laboratories, Elkhart, TN), and sections were cut at 4 μm thickness. Immunohistochemical staining for murine OPN and CD31 was performed as previously described [23]. To quantify apoptotic cell number in the tumor, we performed immunohistochemical staining for ssDNA. Briefly, the sections were fixed with 4% paraformaldehyde (PFA) and then incubated at 4 °C overnight with rabbit anti-ssDNA antibody diluted to 1:400. Specific binding was detected through avidin-biotin peroxidase complex formation with biotin conjugated goat anti-rabbit IgG (Vectastain ABC kit, Vector, Burlingame, CA) and diaminobendizine (DAB) (Sigma, St. Louis, MI) as the substrate. Staining was absent when isotype-matched immunoglobulin was used as the control.

2.12. HUVEC proliferation assay

A 96-well flat bottom plastic assay plate (Corning, NY) was coated with recombinant mouse OPN (RD systems, Inc., CA; 10 μg/ml), polylysine (100 μg/ml) or BSA (10 mg/ml) in PBS and incubated overnight at 4 °C. The plate was washed with PBS and non-specific adhesion sites were blocked with 1% BSA in PBS for 1 h at 37 °C. After washing the wells with PBS, 5×10^3 cells in 100 μl of EGM-2 medium diluted with OPTI-MEM (Invitrogen) to 1/5 were seeded to each well. For some experiments, the HUVEC suspensions were pretreated with GRGDS peptide at the concentration of 100 μM or anti-human αvβ3 antibody at the concentration of 10 μg/ml for 1 h at 37 °C. Then after 48 h incubation, 10 μl of 2-(2-methoxy-4-nitrophenyl)-3-(4-nitrophenyl)-5-(2,4-disulfophenyl)-2H-tetrazolium monosodium salt (WST-8, Dojindo, Kumamoto, Japan) was added to each well. The plate was further incubated at 37 °C for 6 h for color development. Absorbance was measured at 450 nm on a microplate reader with microplate manager (Bio-Rad, Richmond, CA). All experiments were performed in triplicate.

2.13. Statistics

Statistical analysis was performed with analysis of variance (ANOVA). All data are presented as mean ± standard deviation. Differences between means were considered statistically significant at $P < 0.05$.

3. Results

3.1. Generation of stable transfectants that secretes murine OPN

BMGneo-mOPN or BMGneo were transfected into SBC-3 cells. Two OPN transfected SBC-3 clones (SBC-3/OPN#5 and SBC-3/OPN#6) and two control clones (SBC-3/NEO#1 and SBC-3/NEO#3) were constructed. To verify the expression of OPN and VEGF mRNA in transfectants, we conducted RT-PCR for OPN and VEGF, respectively. As shown in Fig. 1A, high levels of OPN mRNA expression were detected in the SBC-3/OPN cells, while there were no detectable expression levels observed in the SBC-3/NEO cells. For VEGF mRNA, there was no difference in the level of expression between SBC-3/OPN and SBC-3/NEO cells. Thus, transfection with OPN gene into SBC-3 cells does not affect the expression of other angiogenic inducers like VEGF mRNA. Secreted OPN protein from transfectants was confirmed with both western blot analysis and ELISA kit (Fig. 1B and C). OPN-transfected clones secreted significant amounts of OPN, while control clones did not. The clone SBC-3/OPN#5 secreted the high-

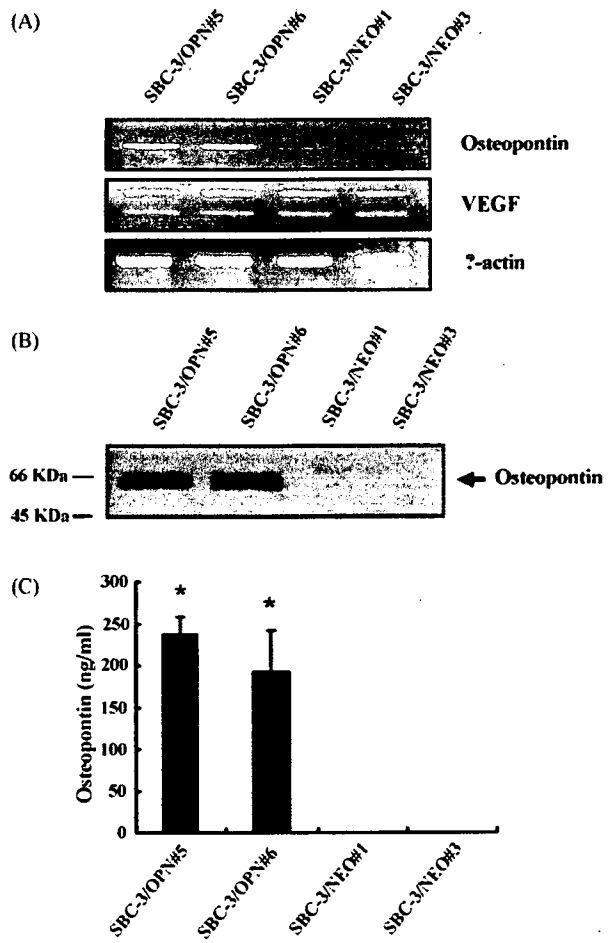

Fig. 1 (A) Expression of OPN and VEGF mRNA determined with RT-PCR analysis. Total RNAs were extracted from each clone and 1 μg of RNAs were subjected to RT-PCR analysis for OPN (top panel), VEGF (middle panel) and β-actin (bottom panel) expression. (B) Western blot analysis of secreted mouse OPN protein. Conditioned mediums from SBC-3/OPN and SBC-3/NEO clones were subjected to western blot analysis using polyclonal antibody against OPN. The arrow indicates the expression of OPN, and molecular standards are shown on the left in KD. (C) Secretion of OPN protein from SBC-3/OPN and SBC-3/NEO cells. Conditioned medium from each clones were collected and subjected to ELISA analysis. Note that the clone SBC-3/OPN#5 secreted the highest level of OPN protein into the culture medium. *$P < 0.05$ vs. SBC-3/NEO#1 and SBC-3/NEO#3.

est level of OPN protein into the culture medium. Therefore, we utilized this clone in the subsequential experiments.

3.2. In vitro cell growth rate of stable OPN-transfectant

Cells were seeded onto 96-well plates and the number of cells was quantified at specific time intervals with MTT assay. Cultured SBC-3/OPN and SBC-3/NEO cells displayed similar in vitro growth rates (data not shown).

3.3. Biological activity of OPN protein secreted from the transfectant

Since endothelial cell migration is essential for tumor angiogenesis, we conducted migration assay using HUVEC. Conditioned medium from SBC-3/OPN cells significantly stimulated HUVEC migration as compared with conditioned medium from SBC-3/NEO cells. Moreover, HUVEC migration toward the culture medium of SBC-3/OPN cells was almost completely suppressed with the addition of GRGDS peptide and anti-human αvβ3 antibody (Fig. 2). These results suggest that OPN secreted from SBC-3/OPN is actually biological active and stimulates HUVEC migration by interacting with αvβ3 integrin.

3.4. Effect of OPN transfection on colony formation

We evaluated whether transfection with OPN gene affects colony formation of SBC-3 cells in vitro with soft agar colony formation assay. As shown in Fig. 2B, there was no significant difference in the number of colonies between SBC-3/OPN and SBC-3/NEO cells. Thus, colony formation of SBC-3 cells in vitro was not affected by transfection with the OPN gene.

3.5. In vivo tumorigenecity of OPN transfectant

To investigate whether OPN has any role in tumor growth in vivo, SBC-3/OPN#5 clone and SBC-3/NEO#1 clone were injected subcutaneously into the left flank of the nude mice. As shown in Fig. 3 A and B, in contrast to the absence of any significant changes in in vitro cell growth, the in vivo growth rate of SBC-3/OPN#5 was significantly faster than that of the SBC-3/NEO#1 cells. We also tested in vivo tumor growth of the other SBC-3/OPN clone, SBC-3/OPN#6, to confirm its enhanced in vivo tumorigenecity. As expected, SBC-3/OPN#6 demonstrated enhanced in vivo tumor growth compared to SBC-3/NEO#1 (data not shown).

3.6. Expression of OPN protein in SBC-3/OPN and SBC-3/NEO tumors

To investigate whether enhanced tumor growth of SBC-3/OPN clones in vivo was mediated by secreted OPN, immunohistochemical staining for OPN was conducted. The OPN-positive cell number was significantly greater in the SBC-3/OPN induced tumor in comparison with that of the SBC-3/NEO tumor (Fig. 3C). These results suggest that

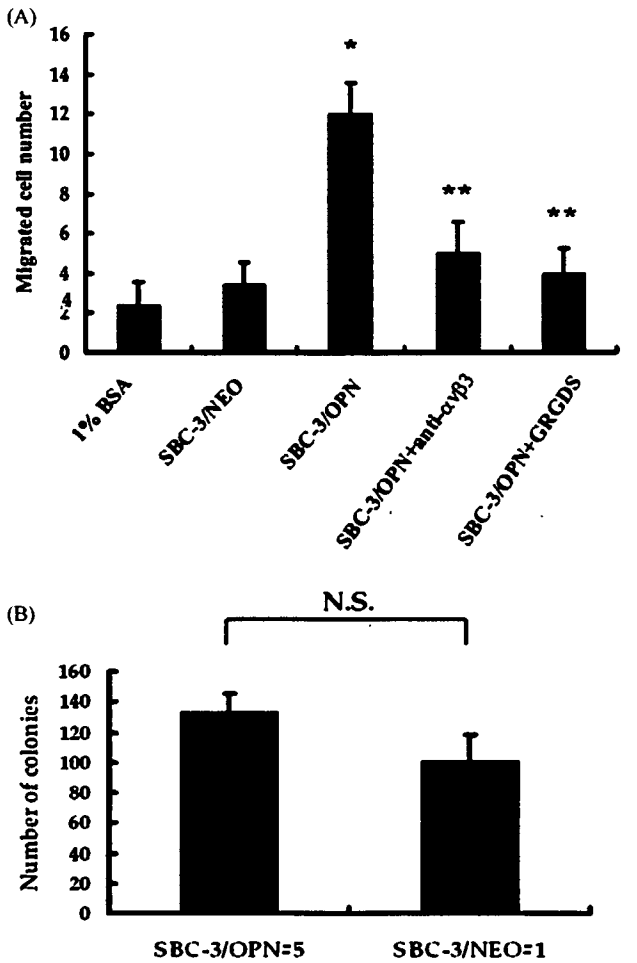

Fig. 2 (A) Migration of HUVEC toward conditioned medium from OPN-transfected cells. Cells were placed in the upper chamber and culture medium from SBC-3/NEO and SBC-3/OPN were added to the lower chamber. After 8 h incubation, cells that migrated through the porous filter were counted at ×200 magnification. Enhanced migration of HUVEC toward the culture medium from SBC-3/OPN was abrogated with the addition of either GRGDS peptide (100 μM) or anti-human αvβ3 antibody (10 μg/ml) to the upper chambers. Data are presented as mean ± S.D. $^{*}P < 0.0001$ vs. 1% BSA and SBC-3/NEO; $^{**}P < 0.001$ vs. SBC-3/OPN. (B) Soft-agar colony formation by SBC-3/OPN and SBC-3/NEO cells. Cells were seeded at an initial density of 5×10^3 cells into 6-well culture plates in triplicate in 0.3% agar. Colonies containing at least 50 cells were scored after 2 weeks of growth. Total colony per well were counted and presented as the mean ± S.D.

secreted OPN from SBC-3/OPN transfectants enhanced in vivo tumorigenesis.

3.7. Effect of OPN transfection on tumor angiogenesis

To investigate whether transfection with OPN gene results in increased tumor angiogenesis in vivo, we performed immunohistochemistry for CD31 and counted the microvessels in the SBC-3/OPN#5 and SBC-3/NEO#1 induced tumors of the nude mice. As shown in Fig. 4A, the number of CD31-

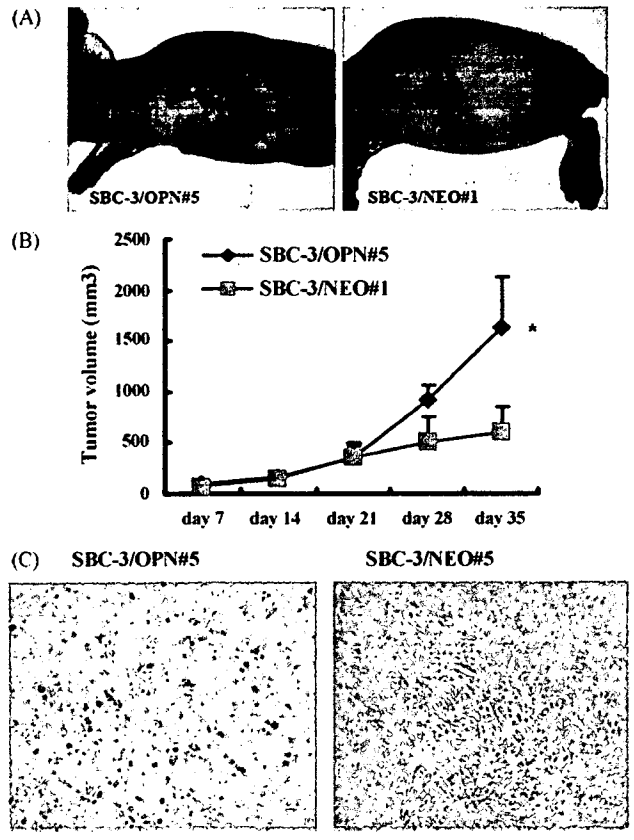

Fig. 3 Effect of OPN gene transfer into SBC-3 cells on tumor growth in mice. The SBC-3/OPN#5 and SBC-3/NEO#1 cells were inoculated s.c. into the left flanks of nude mice. (A) Representative photographs of the tumors at day 35 after inoculation with either the SBC-3/OPN#5 cells or the SBC-3/NEO#1 cells. (B) Tumors were measured with a digital caliper in two perpendicular diameters every week. The tumor volumes were calculated as described in Section 2. Each group consisted of 10 mice. $^{*}P < 0.05$ vs. SBC-3/NEO#1. (C) Representative sections of OPN expression in tumors derived from SBC-3/OPN and SBC-3/NEO. Cryostat sections of tumors developing in nude mice were stained with anti-mouse OPN monoclonal antibody (original magnification ×400).

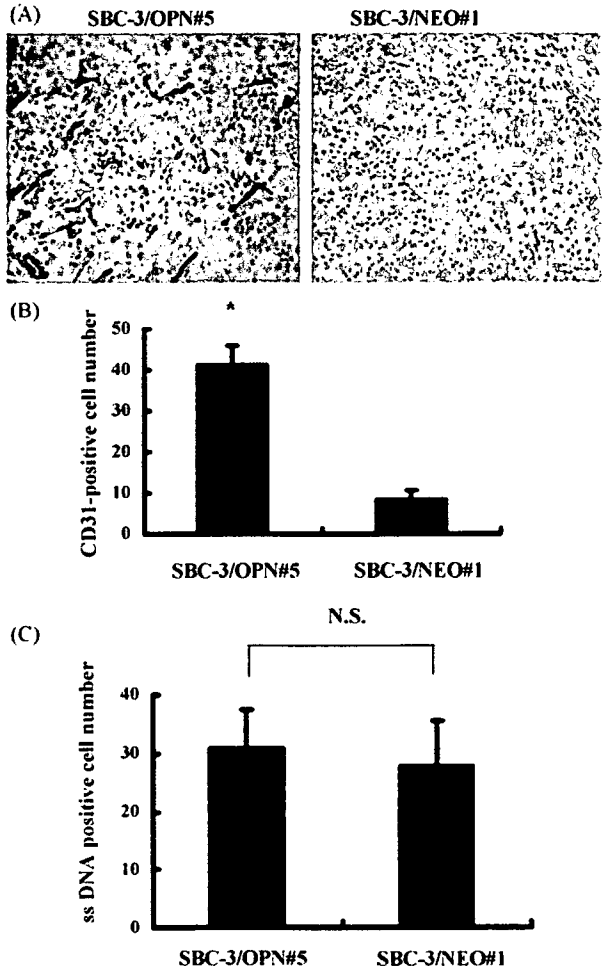

Fig. 4 (A and B) Vascularization of tumors derived from SBC-3/OPN#5 and SBC-3/NEO#1 cells. Cryostat sections of tumors developing in nude mice were stained with anti-CD31 monoclonal antibody. (A) Representative sections were depicted (×200). (B) Quantification of microvessel density in tumors. The number of CD31-positive microvessels in five fields of tumors that demonstrated the highest vascularity was counted at ×200 and presented as mean ± S.D. $^{*}P < 0.001$ vs. SBC-3/NEO#1. (C) Quantification of ss DNA staining in SBC-3/OPN and SBC-3/NEO cells developed in nude mice. The number of ss DNA positive cells in SBC-3/OPN#5 tumor was not significantly different from that of SBC-3/NEO#1 tumor.

positive vascular endothelial cells was markedly increased in the SBC-3/OPN#5 induced tumor compared to that of the SBC-3/NEO#1 induced tumor. As shown in Fig. 4B, greater than tenfold the number of microvessels was identified in the SBC-3/OPN#5 induced tumor compared with the SBC-3/NEO#1 induced tumor. These results strongly imply that OPN upregulates tumor angiogenesis of SBC-3 cells in mice.

3.8. Effect of OPN transfection on tumor cell apoptosis

We evaluated whether transfection with OPN gene affects tumor cell apoptosis of SBC-3 cells in vivo with immunohistochemical staining for ssDNA. As shown in Fig. 4C, the number of apoptotic cells in the SBC-3/OPN induced tumor was not significantly different from that of the SBC-3/NEO induced tumor. These results suggest the apoptosis of SBC-3 cells in vivo was not affected by transfection with the OPN gene.

3.9. Effect of OPN on in vitro HUVEC proliferation

The endothelial cell proliferation is essential for tumor angiogenesis. Therefore, we performed HUVEC proliferation assay using recombinant mouse OPN protein. As shown in Fig. 5, immobilized OPN significantly stimulated HUVEC proliferation compared with immobilized polylysine and BSA. Interestingly, this enhanced HUVEC proliferation mediated by immobilized OPN was significantly inhibited with the addition of anti-human αvβ3 antibody or GRGDS peptide. These results are consistent with our finding that migration of HUVEC to OPN was mediated by αvβ3 integrin as shown in Fig. 2. Taken together, these findings imply the interaction between OPN and αvβ3 integrins on vascular endothelial cells may play an important role in tumor angiogenesis.

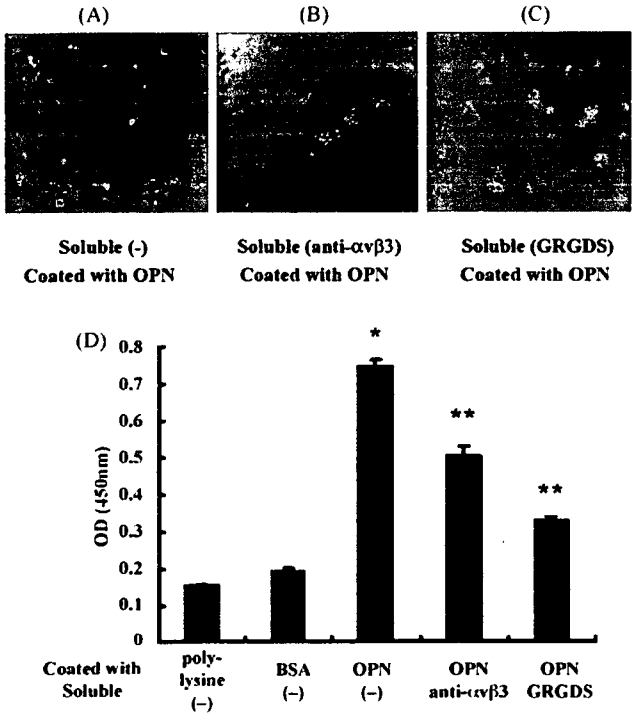

Fig. 5 Inhibitory effect of anti-αvβ3 antibody or RGD peptide on HUVEC proliferation mediated by OPN. (A–C) Representative microphotographs were depicted (×100). (D) Immobilized OPN significantly enhanced HUVEC proliferation and this enhancement was markedly suppressed by treatment with anti-αvβ3 antibody or RGD peptide. Data are presented as mean ± S.D. *$P < 0.0001$ vs. coated with BSA, soluble (−); **$P < 0.001$ vs. coated with OPN, soluble (−).

3.10. Effect of RMV-7 antibody or TNP-470 on growth of SBC-3/OPN tumor in vivo

Since the SBC-3/OPN#5 induced tumors revealed strong neovascularization and tumor growth, the SBC-3/OPN#5 induced tumors were treated with RMV-7 or anti-angiogenic agent, TNP-470, to investigate whether the accelerated SBC-3/OPN#5 tumor growth *in vivo* was directly associated with neovascularization mediated by the interaction between OPN and its receptor, αvβ3 integrin. As shown in Table 1, TNP-470 and RMV-7 administration significantly reduced *in vivo* tumor growth against SBC-3/OPN#5 cells with growth-inhibitory ratio (GIR) values (%) of 83.8% and 85.6%, respectively. In contrast to strong antitumor activity against SBC-3/OPN tumor, RMV-7 did not reveal any antitumor activity against the SBC-3/NEO tumor. These results suggest that the abrogation of the interaction between OPN and αvβ3 integrin could be an effective therapeutic modality in OPN-overexpressing lung cancer.

4. Discussion

OPN is a secreted multifunctional glycosylated phosphoprotein that is involved in tumor progression and metastasis through interaction with adhesion molecules such as integrins αvβ3, αvβ5, and αvβ1, and CD44 variants in a RGD sequence dependent or independent manner [24,25]. Angiogenesis plays a central role in the growth and metastasis of various cancers. The endothelial cell migration is dependent on their adhesive to extracellular matrix protein such as OPN through a variety of cell adhesion receptor including αvβ3 integrins [26]. It has been reported that overexpression of the αvβ3 integrin on tumor vasculature is associated with an aggressive phenotype of several solid tumor types [27,28]. Recent clinical studies also revealed that OPN, a ligand for αvβ3, overexpression is associated with tumor progression and poor survival of patients with lung cancer [17,18].

Table 1 Antitumor activity of RMV-7 or TNP-470 against SBC-3/OPN and SBC-3/NEO inoculated into nude mice

Cell line	Agent	Tumor volume (mm^3)	GIR (%)
SBC-3/OPN#5	TNP-470 (−)	506.9 ± 246.28	83.8
	TNP-470 (+)[b]	81.79 ± 34.4*	
	RMV-7 (−)	2272.45 ± 1126.73	85.6
	RMV-7 (+)[a]	326.35 ± 157.18**	
SBC-3/NEO#1	TNP-470 (−)	126.7 ± 27.98	27.1
	TNP-470 (+)[b]	92.36 ± 12.64	
	RMV-7 (−)	464.76 ± 167.49	3.6
	RMV-7 (+)[a]	448.17 ± 177.68	

Antitumor activity was evaluated in term of growth-inhibitory ratio (GIR, %), defined as [1 − (mean tumor volume of treated/mean tumor volume of control)] × 100 at day 32[a] after the first administration of RMV-7 or day 28[b] after the first administration of TNP-470. Data are presented as mean ± S.D.
* $P < 0.05$ vs. TNP-470 (−).
** $P < 0.05$ vs. RMV-7 (−).

In this study, we conducted *in vivo* tumorigenicity experiments using human lung cancer cell line, SBC-3 cells, to reveal whether interaction between OPN and its receptor αvβ3 plays a key role in tumor growth mediated by angiogenesis. The SBC-3 cell line was originally established from bone marrow aspirate of the 24-year-old male patient with small cell lung cancer [29]. Its subcutaneous implantability has been approved by Fukumoto et al. [30]. OPN-overexpressing SBC-3 cells significantly enhanced *in vivo* tumor growth compared to the control cells. Interestingly, *in vitro* cell growth rate and VEGF mRNA expression levels were similar among these cells. In contrast, transfection of SBC-3 cells with OPN gene significantly induced neovascularization *in vivo*. Apoptosis of SBC-3 cells *in vivo* and colony formation of SBC-3 cells *in vitro* were not affected by transfection with the OPN gene. These results imply that promotion of the tumor growth of SBC-3/OPN cells *in vivo* may be attributed to the hypervascularization induced by secreted OPN. In fact, recombinant human OPN protein enhanced HUVEC proliferation *in vitro*, and these effects of OPN were significantly suppressed with the addition of anti-αvβ3 integrin monoclonal antibody or RGD peptide. These results suggest that OPN is implicated in the process of angiogenesis by interacting with the αvβ3 integrin. In addition, we performed *in vivo* experiment to evaluate the metastatic effect of OPN. The cell suspensions of SBC-3/OPN or SBC-3/NEO cells were injected into a lateral tail vein of BALB/c nude mice. Unfortunately, we did not observe metastatic colonies in lungs. Although liver and kidney metastasis were observed, there

was no significant difference in the number of metastatic colonies in livers and kidneys between in SBC-3/OPN and SBC-3/NEO injected mice (data not shown).

The sustained growth of solid tumors is dependent on the vascular network, making tumor blood vessels a potential therapeutic target [3]. Since previous reports confirmed that OPN plays an important role in tumor progression and metastasis, various therapeutical trials targeting the interaction between OPN and its receptors have been proposed. Thalmann et al. reported that anti-OPN antibody inhibits the growth stimulatory effect of endogenous OPN for human prostate carcinoma cells [31]. In addition, a murine anti-human OPN antibody, which recognizes the RGD/thrombin cleavage region, inhibits the adhesion of MDA-MB-435 breast cancer cells to OPN [32]. Recent trials have used the siRNA technique to knock down OPN mRNA expression. Shevde et al. have demonstrated that suppression of OPN mRNA with siRNA reduced tumorigenecity of MDA-MB-435 breast cancer cells [33]. In addition, Wai et al. revealed that inhibition of OPN mRNA reduced metastatic potential in murine colon carcinoma cells [34]. Regarding anti-OPN receptor antibodies, Brooks et al. have reported that monoclonal antibody (LM609) against αvβ3 integrin induces apoptosis of the proliferative angiogenic blood vessel cells and leads to tumor regression in breast cancer [35]. However, there are no studies with regard to the therapeutic trials targeting OPN and its receptor in lung cancer animal models.

In the present study, we evaluated therapeutic efficacy of anti-αvβ3 integrin antibody (RMV-7) in OPN-overexpressing human lung cancer cells inoculated mice model. Treatment of mice with RMV-7 completely suppressed the *in vivo* tumor growth of SBC-3/OPN with GIR value of 85.6%, while growth rate of SBC-3/NEO *in vivo* was not attenuated by treatment with RMV-7. In the same way, anti-angiogenic agent, TNP-470, exhibited strong anti-tumor activity against SBC-3/OPN tumor with GIR value of 83.8%. These results suggest that interaction between OPN and αvβ3 integrin plays a crucial role for tumor growth induced by up-regulated angiogenesis of human lung cancer cells in mice and anti-αvβ3 antibody could be useful in anti-angiogenic treatment of human lung cancer.

Phase I study using vitaxin (humanized monoclonal anti-αvβ3 integrin antibody) has demonstrated its safety and potential activity in some human cancers. This study revealed that one patient demonstrated partial response and seven patients exhibited stable disease course among the 14 patients evaluated [36]. Recently, McNeel et al. reported phase I trial of a monoclonal antibody specific for αvβ3 integrin (MEDI-522) in patient with advanced multiple malignancies including lung cancer [37]. In their study, three patients with renal carcinoma demonstrated a prolonged and stable disease course among the 25 patients investigated. However, none of the patients with lung cancer revealed favorable therapeutic response. According to our previous report, OPN is predominantly expressed in NSCLC, but its expression level is variable [38]. In both phase I trials, they did not mention the issue of OPN expression in NSCLC. The reason why none of the patients with NSCLC revealed any response to treatment with anti-αvβ3 antibody might have been due to the low expression of OPN in NSCLC cells in these patients. In fact, administration of RMV-7 antibody did not reduce *in vivo* tumor growth in SBC-3/NEO cells inoculated mice in our study. These results suggest that intratumoral OPN expression could be a surrogate marker in the prediction of therapeutic response for treatment with anti-αvβ3 integrin antibody in lung cancer.

Conclusively, our study revealed that OPN is involved in tumor growth and angiogenesis of lung cancer by up-regulating vascular endothelial cell migration and proliferation via interacting with αvβ3 integrin. OPN and its receptor could be effective target molecules in the future for anti-angiogenic therapy of patients with lung cancer.

Conflict of interest

None.

References

[1] Bhattacharjee A, Richards WG, Staunton J, Li C, Monti S, Vasa P, et al. Classification of human lung carcinomas by mRNA expression profiling reveals distinct adenocarcinoma subclasses. Proc Natl Acad Sci USA 2001;98:13790–5.

[2] Chan DC, Earle KA, Zhao TL, Helfrich B, Zeng C, Baron A, et al. Exisulind in combination with docetaxel inhibits growth and metastasis of human lung cancer and prolongs survival in athymic nude rats with orthotopic lung tumors. Clin Cancer Res 2002;8:904–12.

[3] Folkman J. Angiogenesis in cancer, vascular, rheumatoid and other disease. Nat Med 1995;1:27–31.

[4] Folkman J, Shing Y. Angiogenesis. J Biol Chem 1992;267: 10931–4.

[5] Eliceiri BP, Cheresh DA. The role of alphav integrins during angiogenesis: insights into potential mechanisms of action and clinical development. J Clin Invest 1999;103:1227–30.

[6] Varner JA. The role of vascular cell integrins alpha v beta 3 and alpha v beta 5 in angiogenesis. Exs 1997;79:361–90.

[7] Patarca R, Saavedra RA, Cantor H. Molecular and cellular basis of genetic resistance to bacterial infection: the role of the early T-lymphocyte activation-1/osteopontin gene. Crit Rev Immunol 1993;13:225–46.

[8] Takahashi K, Takahashi F, Tanabe KK, Takahashi H, Fukuchi Y. The carboxyl-terminal fragment of osteopontin suppresses arginine-glycine-asparatic acid-dependent cell adhesion. Biochem Mol Biol Int 1998;46:1081–92.

[9] Agrawal D, Chen T, Irby R, Quackenbush J, Chambers AF, Szabo M, et al. Osteopontin identified as lead marker of colon cancer progression, using pooled sample expression profiling. J Natl Cancer Inst 2002;94:513–21.

[10] Chambers AF, Wilson SM, Kerkvliet N, O'Malley FP, Harris JF, Casson AG. Osteopontin expression in lung cancer. Lung Cancer 1996;15:311–23.

[11] Kim JH, Skates SJ, Uede T, Wong KK, Schorge JO, Feltmate CM, et al. Osteopontin as a potential diagnostic biomarker for ovarian cancer. JAMA 2002;287:1671–9.

[12] Tuck AB, Chambers AF. The role of osteopontin in breast cancer: clinical and experimental studies. J Mammary Gland Biol Neoplasia 2001;6:419–29.

[13] Tuck AB, O'Malley FP, Singhal H, Tonkin KS, Harris JF, Bautista D, et al. Osteopontin and p53 expression are associated with tumor progression in a case of synchronous, bilateral, invasive mammary carcinomas. Arch Pathol Lab Med 1997;121:578–84.

[14] Ue T, Yokozaki H, Kitadai Y, Yamamoto S, Yasui W, Ishikawa T, et al. Co-expression of osteopontin and CD44v9 in gastric cancer. Int J Cancer 1998;79:127–32.

[15] Senger DR, Ledbetter SR, Claffey KP, Papadopoulos-Sergiou A, Peruzzi CA, Detmar M. Stimulation of endothelial cell

migration by vascular permeability factor/vascular endothelial growth factor through cooperative mechanisms involving the alphavbeta3 integrin, osteopontin, and thrombin. Am J Pathol 1996;149:293–305.
[16] Shijubo N, Kojima H, Nagata M, Ohchi T, Suzuki A, Abe S, et al. Tumor angiogenesis of non-small cell lung cancer. Microsc Res Tech 2003;60:186–98.
[17] Donati V, Boldrini L, Dell'Omodarme M, Prati MC, Faviana P, Camacci T, et al. Osteopontin expression and prognostic significance in non-small cell lung cancer. Clin Cancer Res 2005;11:6459–65.
[18] Hu Z, Lin D, Yuan J, Xiao T, Zhang H, Sun W, et al. Overexpression of osteopontin is associated with more aggressive phenotypes in human non-small cell lung cancer. Clin Cancer Res 2005;11:4646–52.
[19] Takahashi F, Takahashi K, Okazaki T, Maeda K, Ienaga H, Maeda M, et al. Role of osteopontin in the pathogenesis of bleomycin-induced pulmonary fibrosis. Am J Respir Cell Mol Biol 2001;24:264–71.
[20] Takahashi K, Nakamura T, Koyanagi M, Kato K, Hashimoto Y, Yagita H, et al. A murine very late activation antigen-like extracellular matrix receptor involved in CD2- and lymphocyte function-associated antigen-1-independent killer-target cell interaction. J Immunol 1990;145:4371–9.
[21] Takahashi F, Akutagawa S, Fukumoto H, Tsukiyama S, Ohe Y, Takahashi K, et al. Osteopontin induces angiogenesis of murine neuroblastoma cells in mice. Int J Cancer 2002;98:707–12.
[22] Cui R, Takahashi K, Takahashi F, Tanabe KK, Fukuchi Y. Endostatin gene transfer in murine lung carcinoma cells induces vascular endothelial growth factor secretion resulting in up-regulation of in vivo tumorigenecity. Cancer Lett 2006;232:262–71.
[23] Hirama M, Takahashi F, Takahashi K, Akutagawa S, Shimizu K, Soma S, et al. Osteopontin overproduced by tumor cells acts as a potent angiogenic factor contributing to tumor growth. Cancer Lett 2003;198:107–17.
[24] Brown LF, Papadopoulos-Sergiou A, Berse B, Manseau EJ, Tognazzi K, Perruzzi CA, et al. Osteopontin expression and distribution in human carcinomas. Am J Pathol 1994;145: 610–23.
[25] Weber GF, Ashkar S, Glimcher MJ, Cantor H. Receptor-ligand interaction between CD44 and osteopontin (Eta-1). Science 1996;271:509–12.
[26] Auerbach W, Auerbach R. Angiogenesis inhibition: a review. Pharmacol Ther 1994;63:265–311.
[27] Gasparini G, Brooks PC, Biganzoli E, Vermeulen PB, Bonoldi E, Dirix LY, et al. Vascular integrin alpha(v)beta3: a new prognostic indicator in breast cancer. Clin Cancer Res 1998;4:2625–34.
[28] Mitjans F, Sander D, Adan J, Sutter A, Martinez JM, Jaggle CS, et al. An anti-alpha v-integrin antibody that blocks integrin function inhibits the development of a human melanoma in nude mice. J Cell Sci 1995;108(Pt 8):2825–38.
[29] Miyamoto H. Establishment and characterization of an adriamycin-resistant subline of human small cell lung cancer cells. Acta Med Okayama 1986;40:65–73.
[30] Fukumoto H, Nishio K, Ohta S, Hanai N, Fukuoka K, Ohe Y, et al. Effect of a chimeric anti-ganglioside GM2 antibody on ganglioside GM2-expressing human solid tumors in vivo. Int J Cancer 1999;82:759–64.
[31] Thalmann GN, Sikes RA, Devoll RE, Kiefer JA, Markwalder R, Klima I, et al. Osteopontin: possible role in prostate cancer progression. Clin Cancer Res 1999;5:2271–7.
[32] Bautista DS, Xuan JW, Hota C, Chambers AF, Harris JF. Inhibition of Arg-Gly-Asp (RGD)-mediated cell adhesion to osteopontin by a monoclonal antibody against osteopontin. J Biol Chem 1994;269:23280–5.
[33] Shevde LA, Samant RS, Paik JC, Metge BJ, Chambers AF, Casey G, et al. Osteopontin Knockdown Suppresses Tumorigenicity of Human Metastatic Breast Carcinoma, MDA-MB-435. Clin Exp Metastasis 2006;23:123–33.
[34] Wai PY, Mi Z, Guo H, Sarraf-Yazdi S, Gao C, Wei J, et al. Osteopontin silencing by small interfering RNA suppresses in vitro and in vivo CT26 murine colon adenocarcinoma metastasis. Carcinogenesis 2005;26:741–51.
[35] Brooks PC, Stromblad S, Klemke R, Visscher D, Sarkar FH, Cheresh DA. Antiintegrin alpha v beta 3 blocks human breast cancer growth and angiogenesis in human skin. J Clin Invest 1995;96:1815–22.
[36] Gutheil JC, Campbell TN, Pierce PR, Watkins JD, Huse WD, Bodkin DJ, et al. Targeted antiangiogenic therapy for cancer using Vitaxin: a humanized monoclonal antibody to the integrin alphavbeta3. Clin Cancer Res 2000;6:3056–61.
[37] McNeel DG, Eickhoff J, Lee FT, King DM, Alberti D, Thomas JP, et al. Phase I trial of a monoclonal antibody specific for alphavbeta3 integrin (MEDI-522) in patients with advanced malignancies, including an assessment of effect on tumor perfusion. Clin Cancer Res 2005;11:7851–60.
[38] Zhang J, Takahashi K, Takahashi F, Shimizu K, Ohshita F, Kameda Y, et al. Differential osteopontin expression in lung cancer. Cancer Lett 2001;171:215–22.

Pertuzumab, a novel HER dimerization inhibitor, inhibits the growth of human lung cancer cells mediated by the HER3 signaling pathway

Kazuko Sakai,[1,3] Hideyuki Yokote,[1,4] Kimiko Murakami-Murofushi,[3] Tomohide Tamura,[2] Nagahiro Saijo[2] and Kazuto Nishio[1,4,5]

[1]Shien-Laboratory,[2]Medical Oncology, National Cancer Center Hospital; Tsukiji 5-1-1, Chuo-ku, Tokyo 104-0045; [3]Department of Biology, Faculty of Science, Ochanomizu University, Ohtsuka 2-1-1, Bunkyo-ku, Tokyo 112-8610; [4]Depatment of Genome Biology, Kinki University School of Medicine, 377-2 Ohno-Higashi, Osaka-Sayama, Osaka 589-8511, Japan

(Received December 18, 2006/Revised April 4, 2007/Accepted May 10, 2007/Online publication July 9, 2007)

A humanized anti-HER2 monoclonal antibody pertuzumab (Omnitarg, 2C4), binding to a different HER2 epitope than trastuzumab, is known as an inhibitor of heterodimerization of the HER receptors. Potent antitumor activity against HER2-expressing breast and prostate cancer cell lines has been clarified, but this potential is not clear against lung cancers. The authors investigated the *in vitro* anti-tumor activity of pertuzumab against eight non-small cell lung cancer cells expressing various members of the HER receptors. A lung cancer 11_18 cell line expressed a large amount of HER2 and HER3, and its cell growth was stimulated by an HER3 ligand, heregulin (HRG)-α. Pertuzumab significantly inhibited the HRG-α-stimulated cellular growth of the 11_18 cells. Pertuzumab blocked HRG-α-stimulated phosphorylation of HER3, mitogen-activated protein kinase (MAPK), and Akt. In contrast, pertuzumab failed to block epidermal growth factor (EGF)-stimulated phosphorylation of EGF receptor (EGFR) and MAPK. Immunoprecipitation showed that pertuzumab inhibited HRG-α-stimulated HER2/HER3 heterodimer formation. HRG-α-stimulated HER3 phosphorylation was also observed in the PC-9 cells co-overexpressing EGFR, HER2, and HER3, but the cell growth was neither stimulated by HRG-α nor inhibited by pertuzumab. The present results suggest that pertuzumab is effective against HRG-α-dependent cell growth in lung cancer cells through inhibition of HRG-α-stimulated HER2/HER3 signaling. (*Cancer Sci* 2007; 98: 1498–1503)

The HER family of receptor tyrosine kinases consists of four members: EGFR (also termed HER1/ErbB-1), HER2/ErbB-2/Neu, HER3/ErbB-3, and HER4/ErbB-4.[1] Binding of ligands leads to the homo- and heterodimer formation of the receptor tyrosine kinase.[2] There are numerous HER-specific ligands that generate signaling diversity within the cell.[3] EGF, amphiregulin, and TGF-α are known as a specific ligand of EGFR. HB-EGF, β-cellulin, and epiregulin have dual specificity for binding to EGFR and HER4. HRG-α binds HER3 and HER4.[4] No direct ligand for HER2 has been discovered. Dimerization consequently stimulates the intrinsic tyrosine kinase activity of receptors, and activates the downstream-signaling molecules such as MAPK, Akt, JAK, and STAT.[5,6]

Pertuzumab is a humanized monoclonal antibody and binds to the dimerization domain of HER2 distinct from the domain that trastuzumab binds to.[7] Therefore, pertuzumab is known as a dimerization inhibiter between HER2 and the other HER family receptors. A phase I trial of pertuzumab has been performed for advanced tumors,[8] and phase II studies of pertuzumab are underway. Two members of the HER family, HER2 and HER3, act as key oncogenes in breast cancer cells.[9,10] *In vitro* and *in vivo* anti-tumor activities of pertuzumab have been reported in breast tumors through the inhibition of the HER2/HER3 heterodimer formation.[11,12] In lung cancer cells, EGFR plays a crucial role in their biological behavior, but it is unclear whether pertuzumab inhibits the growth of the lung cancer cells mediated by HER family receptors.

The authors have focused on the growth inhibitory effect of pertuzumab against NSCLC cells expressing different types of HER receptors, and analyzed the mechanism of action of pertuzumab in response to the HER receptor ligand.

Materials and Methods

Reagents. Pertuzumab (Omnitarg, 2C4) was provided in sterile water at 25 mg/mL by Genentech, Inc. (South San Francisco, CA, USA) before use. All chemicals and reagents were purchased from Sigma (St Louis, MO, USA) unless noted otherwise.

Cell lines. The human NSCLC cell lines PC-7, PC-9, and PC-14 (Tokyo Medical University, Tokyo, Japan),[13,14] A549 (American Type Culture Collection, Manassas, VA, USA), and PC-3, Ma-1, Ma-24, and 11_18,[15] were maintained in RPMI 1640 medium supplemented with 10% heat-inactivated FBS (Life Technologies, Rockville, MD, USA).

Cell stimulation and lysis. Cells were starved in serum free RPMI 1640 medium for 24 h and treated with EGF, TGF-α, HB-EGF, and HRG-α at 100 ng/mL for 10 min. Cells were washed twice with ice-cold PBS, and lysed with lysis buffer (50 mM Tris, pH 7.5, 150 mM NaCl, 1% Nonidet P-40, 1 mM EDTA, 5 mM sodium pyrophosphate, 50 mM NaF, 1 mM sodium vanadate, 4 mg/mL leupeptin, 4 mg/mL apoprotein, 1 mM PMSF). Protein concentration of the supernatants was determined by the BCA protein assay (Pierce, Rockford, IL, USA).

Immunoprecipitation. Cell lysates (1000 μg) were incubated with the anti-HER2 antibody (Santa Cruz Biotechnology, Santa Cruz, CA, USA) at 4°C overnight. Protein G magnetic beads (New England BioLabs, Beverly, MA, USA) were added for 2 h. Beads were washed three times with lysis buffer, resuspended in SDS sample buffer with 2% β-mercaptoethanol, boiled, and separated using SDS-PAGE.

Western blotting. Cell lysates were electrophoretically separated on SDS-PAGE and transferred to a polyvinylidene difluoride

[5]To whom correspondence should be addressed. E-mail: knishio@med.kindai.ac.jp

Abbreviations: BCA, bicinchoninic acid; ECL, electrochemiluminescence; EDTA, ethylene diamine tetra-acetic acid; EGF, epidermal growth factor; EGFR, epidermal growth factor receptor; FBS, fetal bovine serum; HB-EGF, heparin-binding epidermal growth factor; HRG-α, heregulin-α; JAK, Janus kinase; MAPK, mitogen-activated protein kinase; MTS, 3-(4,5-dimethylthiazol-2-yl)-5-(3-carboxymethoxyphenyl)-2-(4-sulfophenyl)-2H-tetrazolium; NSCLC, non-small cell lung cancer; PBS, phosphate-buffered saline; PMSF, phenylmethylsulfonyl fluoride; RPMI, Roswell Park Memorial Institute; SDS-PAGE, sodium dodecyl sulfate–polyacrylamide gel electrophoresis; STAT, signal transducer and activator of transcription; TGF-α, transforming growth factor-α.

doi: 10.1111/j.1349-7006.2007.00553.x

membrane (Millipore, Bedford, MA, USA). The membrane was probed with each antibody against EGFR and HER2 (Transduction Laboratory, San Diego, CA, USA), HER3 (Santa Cruz Biotechnology), phospho-EGFR (Tyr1068), phospho-HER3 (Tyr1289), MAPK, phospho-MAPK (Thr202/204), Akt, phospho-Akt (Ser473) (Cell Signaling, Beverly, MA, USA), phosphotyrosine (PY-20, Transduction Laboratory), and β-actin (Sigma) as the first antibody, followed by detection using a horseradish peroxidase-conjugated secondary antibody. The bands were visualized with ECL (Amersham, Piscataway, NJ, USA), and images of blotted patterns were analyzed with NIH image software (National Institutes of Health, Bethesda, MD, USA).

Growth inhibition assay. A 100-μL volume of cell suspension (5000 cells/well) in serum-free RPMI 1640 medium was seeded into a 96-well plate and 50 μL of each drug at various concentrations and 50 μL of EGF, TGF-α, HB-EGF, and HRG-α, at 100 ng/mL was added. Human IgG1 (Calbiochem, Cambridge, MA, USA) was used as isotype control. After incubation for 72 h at 37°C, 20 μL of MTS solution (Promega, Madison, WI, USA) was added to each well and the plates were incubated for a further 2 h at 37°C. The absorbance readings for each well were determined at 490 nm with a Delta-soft on a Macintosh computer (Apple, Cupertino, CA, USA) interfaced to a Bio-Tek Microplate Reader EL-340 (BioMetallics, Princeton, NJ, USA). For ligand-stimulated growth of cells, the experiment was performed in six replicate wells for each ligand and carried out independently three times. For growth inhibition of pertuzumab, the experiment was performed in three replicate wells for each drug concentration and carried out independently three times as described elsewhere.[16]

Results

HRG-α dependent cell growth in lung cancer cells. Ligand-dependent cell growth of lung cancer cells was examined (Fig. 1). The addition of EGF, TGF-α, and HB-EGF increased the cell growth of the PC-3, 11_18, and A549 cells, but not that of the PC-7, PC-9, PC-14, Ma-1, and Ma-24 cells. HRG-α addition significantly increased the growth of the 11_18 cells (390% of control, $P < 0.01$ by t-test) and Ma-24 cells (204% of control, $P < 0.01$ by t-test), but did not influence the growth of any other cells. These findings suggest that the growth of the 11_18 and Ma-24 cells is depending upon HRG-α.

Pertuzumab inhibits HRG-α-dependent cell growth of the 11_18 and Ma-24 cells. Pertuzumab inhibited cell growth stimulated by HRG-α (IC_{50} = 0.12 μg/mL) but not stimulated by EGF, TGF-α, and HB-EGF in the 11_18 cells (IC_{50} > 100 μg/mL; Fig. 2). Pertuzumab also inhibited HRG-α dependent cell growth in the Ma-24 cells (IC_{50} = 39.8 μg/mL). Isotype control human IgG1 had no effect on ligand-dependent growth in the 11_18 and Ma-24 cells (data not shown). The growth of the other cells was not affected by exposure to pertuzumab (data not shown). This finding suggests that pertuzumab selectively inhibits HRG-α-dependent cell growth.

Ligand-stimulated phosphorylation of HER receptors. The expression levels of the HER receptors in the pertuzumab-sensitive (11_18 and Ma-24 cells) and pertuzumab-resistant cell (PC-9 cells) lines were determined using western blotting (Fig. 3a). Comparison of the protein expression levels of EGFR revealed high to moderate expression in the PC-9 and Ma-24 cells. EGFR was also detected in the 11_18 cells, although the expression in this

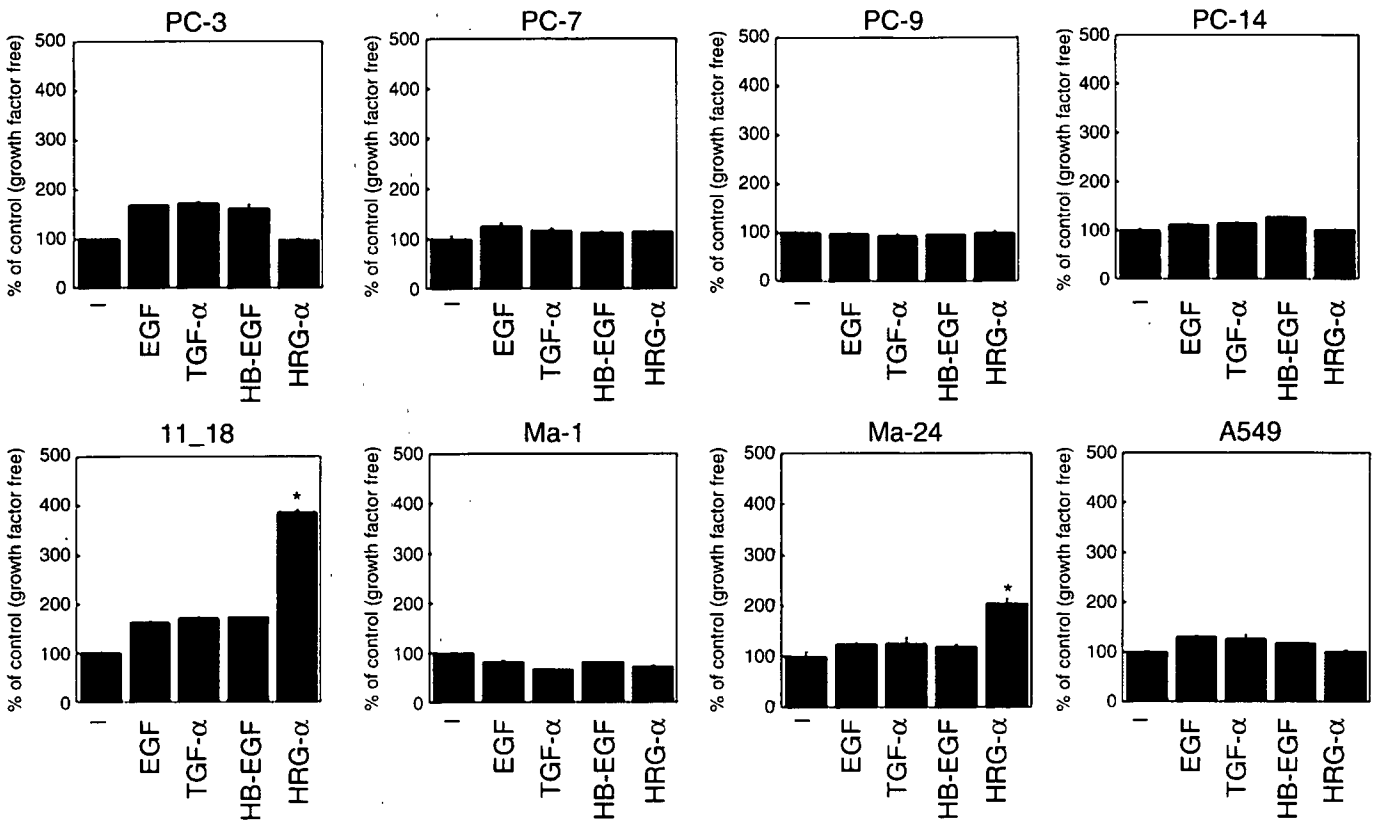

Fig. 1. Ligand-dependent cell growth in the lung cancer cells. Non-small cell lung cancer cells were stimulated with or without 100 ng/mL of epidermal growth factor (EGF), transforming growth factor (TGF)-α, heparin-binding epidermal growth factor (HB-EGF), and heregulin (HRG)-α. After incubation for 72 h, cell growth was determined using the MTS assay. The growth of cells was presented as the percentage of absorbance compared with ligand-untreated cells. Error bars represent SE. *Significant difference ($P < 0.01$; t-test) compared to the ligand-non-stimulated cells. Data shown are representative of at least three independent experiments with similar results.

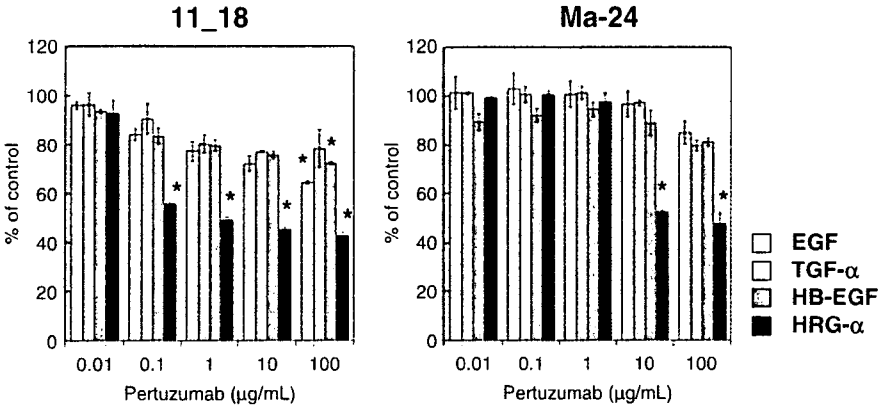

Fig. 2. Growth inhibitory effect of pertuzumab in the lung cancer cells. The lung cells were exposed to pertuzumab (0.01–100 μg/mL) for 72 h in serum free medium with or without 100 ng/mL of epidermal growth factor (EGF), transforming growth factor (TGF)-α, heparin-binding epidermal growth factor (HB-EGF), or heregulin (HRG)-α. The viability was determined using the MTS assay. Result are presented as the percentage of absorbance compared with pertuzumab-untreated cells. Error bars represent SE. *Significant difference ($P < 0.01$; *t*-test) compared to pertuzumab-untreated cells. Data shown are representative of at least three independent experiments with similar results.

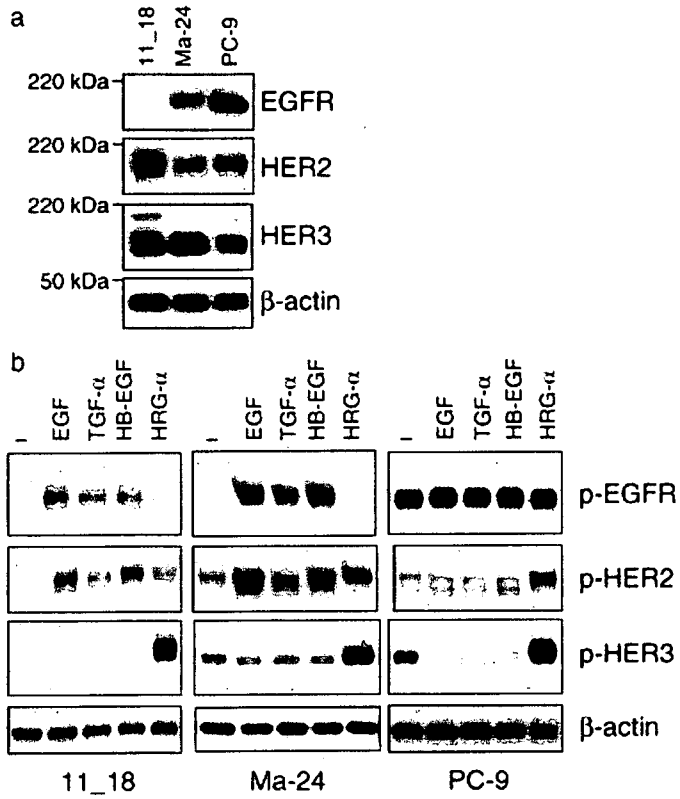

Fig. 3. Expression and phosphorylation of HER receptors in non-small cell lung cancer cells. (a) Expression of epidermal growth factor receptor (EGFR), HER2, and HER3 was detected using western blot analysis. Each lane contained 20 μg protein. β-Actin was used as a loading control. (b) The cells were stimulated with or without 100 ng/mL of epidermal growth factor (EGF), transforming growth factor (TGF)-α, heparin-binding epidermal growth factor (HB-EGF), and heregulin (HRG)-α for 10 min. Phosphorylation of EGFR and HER3 was detected using western blot analysis. Phosphorylation of HER2 was detected using immunoprecipitation followed by western blotting. β-Actin was used as a loading control. Data shown are representative of at least two independent experiments with similar results.

cell line was weak. The expression levels of HER2 were higher in the PC-9 and 11_18 cells than in the Ma-24 cells, which only expressed moderate levels of this receptor. All three cell lines showed strong expression of HER3. HER4 could not be detected in any of the three cell lines (data not shown). In contrast, these lung cancer cell lines expressed different types of EGFR mutations; the PC-9 cells had a 15-base deletion mutant (delE746-A750, exon 19), the 11_18 cells had a L858R point mutation (exon 21) of EGFR, and the Ma-24 cells had a E709G point mutation (exon 18) of EGFR. No mutations were detected in exons 19–21 of HER2 (data not shown).

Next, the ligand-stimulated phosphorylation of the HER receptors in the lung cancer cells after serum starvation was examined (Fig. 3b). While the ligands for EGFR (EGF, TGF-α, and HB-EGF) phosphorylated cellular EGFR in the 11_18 and Ma-24 cells, the EGFR in the PC-9 cells was hyperphosphorylated even under the non-stimulated condition, because PC-9 cells express an active mutant of EGFR. These results suggest that the EGF/TGF-α or HB-EGF–EGFR signals are active in lung cancer cells. The ligands for HER3 (HRG-α) specifically phosphorylated HER3 in the 11_18, Ma-24, and PC-9 cells. Phosphorylation of HER2 was analyzed by immunoprecipitation using an anti-HER2 antibody followed by western blotting for phosphotyrosine. The ligands for EGFR and HER3 phosphorylated HER2 in the 11_18 and Ma-24 cells, whereas only HRG-α but not the other ligands specifically phosphorylated HER2 in the PC-9 cells. These findings also suggest that the HRG-α–HER3 signal is active in lung cancer cells.

Pertuzumab blocks HRG-α but not EGF-stimulated signals. An inhibitory effect of pertuzumab on HRG-α-dependent cell growth in the 11_18 cells was demonstrated. To examine the effect of pertuzumab on signal transduction of both EGFR and HER3 in this cell line, the 11_18 cells were exposed to pertuzumab (0.2–200 μg/mL for 6 h) (Fig. 4a,b). HRG-α-stimulated phosphorylation of HER3 was dose-dependently inhibited by exposure to pertuzumab in the 11_18 cells, whereas EGFR phosphorylation was not stimulated by HRG-α stimulation (data not shown). MAPK and Akt were phosphorylated by HRG-α stimulation and these were inhibited by pertuzumab dose-dependently in the 11_18 cells. In contrast, EGF-stimulated phosphorylation of EGFR and MAPK was not inhibited by pertuzumab in the 11_18 cells. Phosphorylation of Akt was not detected by addition of EGF in the 11_18 cells. EGF did not phosphorylate HER3 and pertuzumab did not affect it (data not shown). Taken together, these results showed that pertuzumab inhibited HRG-α-stimulated phosphorylation of HER3, MAPK, and Akt, but not EGF-stimulated EGFR phosphorylation signaling.

HER3 is phosphorylated in response to HRG-α in the PC-9 cells as observed in the 11_18 cells, but the growth of the PC-9 cells was not increased by HRG-α (Figs 1,3b). To clarify the phosphorylation-inhibitory potential of pertuzumab, the effect of pertuzumab on signal transduction of the PC-9 cells was examined (Fig. 4c). When the PC-9 cells were stimulated by the addition of HRG-α, HER3 was phosphorylated in the PC-9 cells, but phosphorylation of HER3 was not inhibited by pertuzumab (20 and 200 μg/mL for 6 h). EGFR expressed in the PC-9 cells is constitutively active and pertuzumab failed to affect

doi: 10.1111/j.1349-7006.2007.00553.x

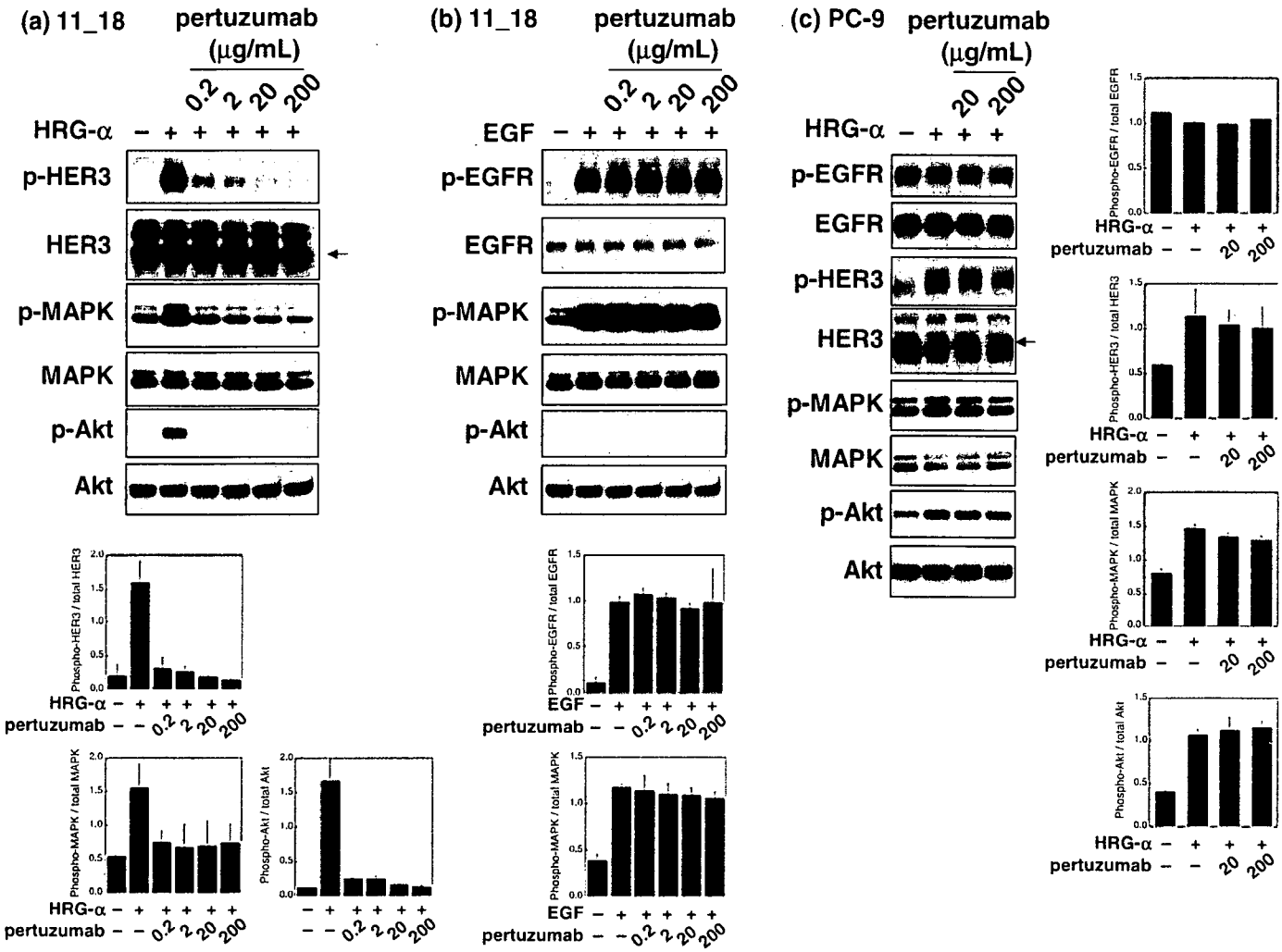

Fig. 4. Effect of pertuzumab on epidermal growth factor receptor (EGFR) and HER3 phosphorylation and their downstream signaling pathways. The 11_18 and PC-9 cells were exposed to pertuzumab for 6 h and stimulated with either heregulin (HRG)-α or epidermal growth factor (EGF) for 10 min. Cell lysate were separated using sodium dodecyl sulfate–polyacrylamide gel electrophoresis and immunoblotted for indicated antibodies. The intensities of bands were quantified by densitometer. (a) HRG-α-stimulated 11_18 cells. (b) EGF-stimulated 11_18 cells. (c) HRG-α-stimulated PC-9 cells. Data shown are representative of at least two independent experiments with similar results. MAPK, mitogen-activated protein kinase.

the phosphorylation level of the EGFR. Phosphorylation of MAPK and Akt was detected by the addition of HRG-α, but these were not inhibited by pertuzumab. These results suggest that pertuzumab is unable to affect HRG-α-stimulated phosphorylation of HER3 in the PC-9 cells.

To clarify the effect of pertuzumab on HER2 phosphorylation and HER2/HER3 heterodimer formation, cell lysates were immunoprecipitated with anti-HER2 antibody (Fig. 5a,b). HRG-α stimulation increased HER2/HER3 heterodimer formation in the 11_18 cells, and pertuzumab decreased HRG-α-stimulated heterodimer formation. EGFR/HER2 heterodimer formation could be barely detected by HRG-α stimulation because of slight expression of EGFR in the 11_18 cells. In the case of EGF stimulation, HER2/HER3 heterodimer was not increased in the 11_18 cells. These findings suggest that pertuzumab inhibits HER2/HER3 heterodimerization by HRG-α stimulation. The HRG-α-stimulated phosphorylation of HER2 was inhibited by pertuzumab in the 11_18 cells. In contrast, the EGF-stimulated phosphorylation of HER2 was not inhibited. These data suggest that pertuzumab inhibits HRG-α stimulated phosphorylation in 11_18 cells. In the PC-9 cells, HRG-α stimulated HER2/HER3 heterodimer formation could be detected without any ligand stimulation, and pertuzumab diminished HRG-α-stimulated heterodimer formation (Fig. 5c). Phosphorylation of HER2 was increased by HRG-α stimulation, but not inhibited by pertuzumab in PC-9 cells. EGFR/HER2 heterodimer formation could be detected without any ligand stimulation, but pertuzumab did not affect it. Based on these results, it is speculated that the cell growth of the PC-9 cells is predominantly dependent on active EGFR signaling, and phosphorylation of HER3 is maintained by active mutant EGFR.

Discussion

Overexpression of HER3 was observed in the lung cancer cell lines and the HER3 was phosphorylated by the HER3 ligand in these cells. These results suggest that HER3 signaling is active in some types of lung cancer cells. Recently it was reported that high HER3 expression was associated with decreased survival.[17] A relationship between lung cancer metastasis and the expression of HER3 as well as EGFR and HER2 has been reported.[18] These bodies of evidence suggest that HER2/HER3 signaling is activated in a subpopulation of lung cancers and that HER2 and HER3 play an important role in the biological behavior of these lung cancers. Both HER2 and HER3 are therefore considered as a possible important target in the therapeutic strategy against lung cancer, just as they are in breast cancers.

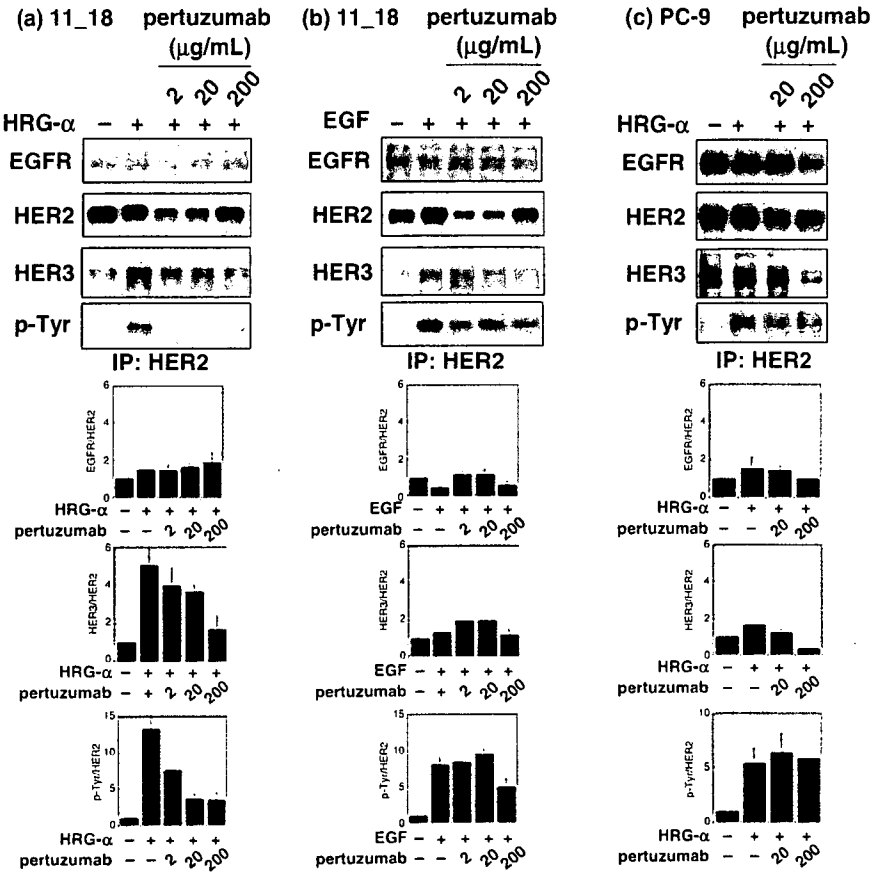

Fig. 5. Effect of pertuzumab on heterodimer formation. The 11_18 and PC-9 cells were exposed to pertuzumab for 6 h and stimulated with either heregulin (HRG)-α or epidermal growth factor (EGF) for 10 min. Cell lysates were immunoprecipitated with anti-HER2 antibody, separated using sodium dodecyl sulfate–polyacrylamide gel electrophoresis, and blotted for indicated antibodies. The intensities of bands were quantified by densitometer. (a) HRG-α-stimulated 11_18 cells. (b) EGF-stimulated 11_18 cells. (c) HRG-α-stimulated PC-9 cells. Data shown are representative of at least two independent experiments with similar results.

HER3 lacks kinase activity because of several base substitutions in motifs that are essential to tyrosine kinase and heterodimerization with HER2 or EGFR is essential for its signal transduction. Therefore co-expression of HER3 and its partners are determinants for the cellular sensitivity against pertuzumab in cancer cells. The present results showed that HER2/HER3 heterodimers are detected by HRG-α stimulation and these data are consistent with previous reports.[19] In contrast, the authors monitored the downstream phosphorylation signal, and demonstrated that HRG-α, but not EGF, phosphorylated Akt in the 11_18 cells. This finding allows us to speculate that HRG-α stimulation leads to Akt phosphorylation through HER2/HER3 heterodimerization.[20–22]

Recently, EGFR mutations have been reported in lung cancers and it was of great interest to clarify the relationship between the EGFR mutation and sensitivity to EGFR-targeted tyrosine kinase inhibitors.[23–25] The PC-9 cells express the deletional mutant EGFR (delE746-A750 in exon 19 of EGFR),[16,23,26,27] and their EGFR was constitutively phosphorylated under non-stimulated conditions (Fig. 3a). The authors speculate that the cell growth of the PC-9 cells is predominantly dependent on active EGFR signaling. In Fig. 3b, treatment with EGF and TGF-α seemed to decrease the phosphorylation of HER3 in PC-9 cells. Unfortunately, we could not conclusively explain this phenomenon. PC-9 cells express deletional EGFR and form EGFR homodimers in the absence of ligand stimulation. At the same time, phospho-HER3 was also detected under these conditions, suggesting that heterodimers of EGFR–HER3 were also formed. Ligand stimulation may alter the balance between homodimers and heterodimers, causing a reduction in HER3 phosphorylation, although there is not any evidence to support this hypothesis. In contrast, the phosphorylation of EGFR in the 11_18 cells that express a different type of mutant EGFR (L858R in exon 21 of EGFR),[26] was not constitutive. This finding may be explained by the differences between deletion mutant EGFR and L858R; constitutive active in the deletion mutant versus hyper-response to ligand stimulation in L858R.[28] Engelman *et al.* suggested that the mutant EGFR is used to couple HER3 in gefitinib-sensitive NSCLC cell lines.[29] The expression level of EGFR in the 11_18 cells was much lower than in the PC-9 cells, and a similar extent of HER3 expression was observed in these cell lines (Fig. 3a). The authors have demonstrated the differential inhibitory effect of pertuzumab against 11_18 and the PC-9 cells. Pertuzumab inhibited HER2/HER3 heterodimer formation and phosphorylation in the 11_18 cells, considering that mutant EGFR do not influence HER3 signals in the 11_18 cells. HER3 phosphorylation in the PC-9 cells was also increased by HRG-α stimulation. Although pertuzumab decreased HER2/HER3 heterodimer formation, it failed to inhibit HRG-α-stimulated HER3 phosphorylation, speculating that an active mutant EGFR transactivates HER3 in the PC-9 cells.

Several EGFR-targeted small inhibitors and antibodies have been under clinical evaluation in the treatment of lung cancer. An EGFR-targeted tyrosine kinase inhibitor, erlotinib, has been clinically applied as a second or third-line single agent therapy in NSCLC patients who have failed standard chemotherapy.[30] Anti-EGFR monoclonal antibodies such as cetuximab and ABX-EGF have been examined in a clinical study.[31] In addition to EGFR, HER2 and HER3 are also considered as important targeting molecules in lung cancers. The present results indicated that pertuzumab effectively inhibited signaling within HER2 and HER3, and may thus be effective in lung cancers expressing HER2 and HER3. To confirm the pertuzumab-sensitive population of lung cancer cells, experiments using small interfering RNA for mutant EGFR will be necessary in future studies.

doi: 10.1111/j.1349-7006.2007.00553.x

In conclusion, the authors have demonstrated that pertuzumab inhibits HRG-α-stimulated cell growth in lung cancer cells through the inhibition of HRG-α-stimulated HER3 signaling. It was further demonstrated that pertuzumab exerts an antiproliferative activity against lung cancer cells expressing HER2 and HER3. The next step will be to examine the clinical relevance of the occurrence of heterodimer formation between HER2 and the other HER receptors in lung cancer.

Acknowledgment

This work was supported by funds for the Third Term Comprehensive 10-Year Strategy for Cancer Control.

References

1 Yarden Y, Sliwkowski MX. Untangling the ErbB signalling network. *Nat Rev Mol Cell Biol* 2001; **2**: 127–37.
2 Tanner KG, Kyte J. Dimerization of the extracellular domain of the receptor for epidermal growth factor containing the membrane-spanning segment in response to treatment with epidermal growth factor. *J Biol Chem* 1999; **274**: 35 985–90.
3 Riese DJ 2nd, Stern DF. Specificity within the EGF family/ErbB receptor family signaling network. *Bioessays* 1998; **20**: 41–8.
4 Chang H, Riese DJ 2nd, Gilbert W, Stern DF, McMahan UJ. Ligands for ErbB-family receptors encoded by a neuregulin-like gene. *Nature* 1997; **387**: 509–12.
5 Park OK, Schaefer TS, Nathans D. *In vitro* activation of Stat3 by epidermal growth factor receptor kinase. *Proc Natl Acad Sci USA* 1996; **93**: 13 704–8.
6 Chang L, Karin M. Mammalian MAP kinase signalling cascades. *Nature* 2001; **410**: 37–40.
7 Franklin MC, Carey KD, Vajdos FF, Leahy DJ, de Vos AM, Sliwkowski MX. Insights into ErbB signaling from the structure of the ErbB2-pertuzumab complex. *Cancer Cell* 2004; **5**: 317–28.
8 Agus DB, Gordon MS, Taylor C *et al.* Phase I clinical study of pertuzumab, a novel HER dimerization inhibitor, in patients with advanced cancer. *J Clin Oncol* 2005; **23**: 2534–43.
9 Slamon DJ, Godolphin W, Jones LA *et al.* Studies of the HER-2/neu proto-oncogene in human breast and ovarian cancer. *Science* 1989; **244**: 707–12.
10 Naidu R, Yadav M, Nair S, Kutty MK. Expression of c-erbB3 protein in primary breast carcinomas. *Br J Cancer* 1998; **78**: 1385–90.
11 Agus DB, Akita RW, Fox WD *et al.* Targeting ligand-activated ErbB2 signaling inhibits breast and prostate tumor growth. *Cancer Cell* 2002; **2**: 127–37.
12 Nahta R, Hung MC, Esteva FJ. The HER-2-targeting antibodies trastuzumab and pertuzumab synergistically inhibit the survival of breast cancer cells. *Cancer Res* 2004; **64**: 2343–6.
13 Nishio K, Arioka H, Ishida T *et al.* Enhanced interaction between tubulin and microtubule-associated protein 2 via inhibition of MAP kinase and CDC2 kinase by paclitaxel. *Int J Cancer* 1995; **63**: 688–93.
14 Kawamura-Akiyama Y, Kusaba H, Kanzawa F, Tamura T, Saijo N, Nishio K. Non-cross resistance of ZD0473 in acquired cisplatin-resistant lung cancer cell lines. *Lung Cancer* 2002; **38**: 43–50.
15 Sato M, Takahashi K, Nagayama K *et al.* Identification of chromosome arm 9p as the most frequent target of homozygous deletions in lung cancer. *Genes Chromosomes Cancer* 2005; **44**: 405–14.
16 Koizumi F, Shimoyama T, Taguchi F, Saijo N, Nishio K. Establishment of a human non-small cell lung cancer cell line resistant to gefitinib. *Int J Cancer* 2005; **116**: 36–44.
17 Yi ES, Harclerode D, Gondo M *et al.* High c-erbB-3 protein expression is associated with shorter survival in advanced non-small cell lung carcinomas. *Mod Pathol* 1997; **10**: 142–8.
18 Muller-Tidow C, Diederichs S, Bulk E *et al.* Identification of metastasis-associated receptor tyrosine kinases in non-small cell lung cancer. *Cancer Res* 2005; **65**: 1778–82.
19 Sliwkowski MX, Schaefer G, Akita RW *et al.* Coexpression of erbB2 and erbB3 proteins reconstitutes a high affinity receptor for heregulin. *J Biol Chem* 1994; **269**: 14 661–5.
20 Graus-Porta D, Beerli RR, Daly JM, Hynes NE. ErbB-2, the preferred heterodimerization partner of all ErbB receptors, is a mediator of lateral signaling. *Embo J* 1997; **16**: 1647–55.
21 Hellyer NJ, Kim MS, Koland JG. Heregulin-dependent activation of phosphoinositide 3-kinase and Akt via the ErbB2/ErbB3 co-receptor. *J Biol Chem* 2001; **276**: 42 153–61.
22 Jackson JG, St Clair P, Sliwkowski MX, Brattain MG. Blockade of epidermal growth factor- or heregulin-dependent ErbB2 activation with the anti-ErbB2 monoclonal antibody 2C4 has divergent downstream signaling and growth effects. *Cancer Res* 2004; **64**: 2601–9.
23 Arao T, Fukumoto H, Takeda M, Tamura T, Saijo N, Nishio K. Small in-frame deletion in the epidermal growth factor receptor as a target for ZD6474. *Cancer Res* 2004; **64**: 9101–4.
24 Lynch TJ, Bell DW, Sordella R *et al.* Activating mutations in the epidermal growth factor receptor underlying responsiveness of non-small-cell lung cancer to gefitinib. *N Engl J Med* 2004; **350**: 2129–39.
25 Paez JG, Janne PA, Lee JC *et al.* EGFR mutations in lung cancer: correlation with clinical response to gefitinib therapy. *Science* 2004; **304**: 1497–500.
26 Nagai Y, Miyazawa H, Huqun *et al.* Genetic heterogeneity of the epidermal growth factor receptor in non-small cell lung cancer cell lines revealed by a rapid and sensitive detection system, the peptide nucleic acid-locked nucleic acid PCR clamp. *Cancer Res* 2005; **65**: 7276–82.
27 Sakai K, Arao T, Shimoyama T *et al.* Dimerization and the signal transduction pathway of a small in-frame deletion in the epidermal growth factor receptor. *Faseb J* 2005; **20**: 311–13.
28 Sordella R, Bell DW, Haber DA, Settleman J. Gefitinib-sensitizing EGFR mutations in lung cancer activate anti-apoptotic pathways. *Science* 2004; **305**: 1163–7.
29 Engelman JA, Janne PA, Mermel C *et al.* ErbB-3 mediates phosphoinositide 3-kinase activity in gefitinib-sensitive non-small cell lung cancer cell lines. *Proc Natl Acad Sci USA* 2005; **102**: 3788–93.
30 Cohen MH, Johnson JR, Chen YF, Sridhara R, Pazdur R. FDA drug approval summary: erlotinib (Tarceva) tablets. *Oncologist* 2005; **10**: 461–6.
31 Govindan R. Cetuximab in advanced non-small cell lung cancer. *Clin Cancer Res* 2004; **10**: 4241–4s.